Benefits of Superconducting Technology to Wireless CDMA Networks

M.I. Salkola[1] and D.J. Scalapino[2]
[1]*Superconductor Technologies Inc., 460 Ward Drive, Santa Barbara, CA 93111*
[2]*Department of Physics, University of California, Santa Barbara, CA 93106*
(May 9, 2003)

***Abstract*— Compact thin-film high-temperature superconducting filters have high selectivity and sensitivity. Combined with a cryocooled, low-noise amplifier, they significantly reduce the effective noise factor of a cellular base-station receiver. Their impact on wireless CDMA networks is examined using a mean-field analysis and numerical simulations. Potential benefits of superconducting technology include increased capacity utilization, coverage efficiency, and data rates. Numerical simulations also address the question of how the network should be optimized to realize these benefits.**

***Index Terms*— Code division multiaccess, CDMA2000, high-temperature superconductors, simulation, and modeling.**

I. Introduction

The rapidly growing demands for wireless communication stress the capabilities of existing systems and the designs of future systems. To meet this challenge, advanced network signal processing algorithms and new hardware are being developed. One new hardware development is the use of thin-film high-temperature superconductors (HTS) and cryocooled, low-noise amplifiers (LNA) to reduce the system noise factor of wireless base-station receivers. Here we examine the potential benefits that this hardware can bring to a Code-Division Multiple-Access (CDMA) network.

The basic function of the crycooled receiver front end, which contains the HTS filter and the LNA, is to remove out-of-band signal power and amplify in-band signals with a minimum degradation of the signal-to-noise ratio. The reduction in the system noise factor of the base-station receiver associated with the introduction of the HTS front end arises from three factors. First, the decrease in insertion loss and the lower operating temperature of the HTS filter significantly lowers the noise factor of the filter. Second, the low-noise amplifier operating in the cryogenic environment adds only a small amount of noise and its gain effectively eliminates the in-band noise contribution from the rest of the receiver. Third, the high selectivity of the HTS filter removes out-of-band signals, which would typically generate intermodulation-distortion (IMD) noise due to the nonlinearities in the rest of the receiver chain and increase the effective noise factor of the receiver.

For the purposes of the CDMA benefit analysis, the properties of the cryocooled front end can be characterized by the effective noise factor F of the base-station receiver [1]. The CDMA analysis shows that for a given situation the dB reduction of the noise factor is equal to the dB reduction in the handset power when the HTS unit is put in place [2]. Thus, other things being equal, an HTS system will reduce handset transmit power leading to longer battery life. More generally, for systems which are reverse-link [3] limited, the deduction in the handset transmit power can be traded off for other network improvements: both the mean-field and numerical simulations show that the HTS unit increases capacity utilization for a given coverage, increases coverage for a given capacity utilization, fills coverage holes, and enables higher reverse-link data transmission rates. The numerical simulations also show the benefits of HTS for call blocking and dropping as well as the need for proper optimization of the network to realize these benefits. Here we extend our previous analysis on HTS benefits that also examined the preliminary experimental evidence for the theory [1].

We begin in Section II by discussing the noise factor of the HTS-filter-LNA receiver. It is the reduction in the system noise factor of the receiver that determines the benefit of the HTS system. In Section III, we briefly review various CDMA mean-field relations [4] for the coverage and capacity from a noise-factor point of view in order to clearly show how a reduction in noise factor can benefit the network. This approach assumes a deterministic traffic load and perfect power control. In Section IV, the results are generalized to take into account fluctuations that arise from the fact that power control is not perfect, IMD noise can be present, and the offered traffic is a random process. Then, in Section V, we turn to a discussion of a numerical simulation which allows us to go beyond the mean-field results and examine the role of the forward link and its effect on the benefits to the network performance that can be realized.

In Section VI, we extend our analysis to discuss the effects of an HTS front end on CDMA2000. This third generation system is designed to provide increased data rates as well as a wide variety of services and exhibits a significant performance benefit from a reduction in the receiver noise factor. In the concluding Section VII, we summarize what our analysis has found regarding the benefits that superconducting technology brings to wireless CDMA networks. We note that various CDMA relations can be written in a robust way which uses directly measurable quantities to characterize the HTS benefit. We point out that our numerical simulations support these analytical relationships as well as allow us to extend them.

II. HTS Filtering

The purpose of an HTS filter is to provide high selectivity with low insertion loss over a desired pass band. The high selectivity removes out-of-band signal strength that would have been mixed into the band of interest by the nonlinear intermodulation of amplifiers and mixers further down the receiver chain. The low insertion loss means that very little of the desired signal is lost passing through the filter and its low operating temperature combined with this low loss means that only a small amount of thermal noise is added. The low-temperature environment required for the HTS filter can also be used to hold an LNA whose gain can mitigate the noise introduced by the remaining part of the receiver chain.

The enhanced performance of cellular system utilizing an HTS filter and LNA front end can be characterized in terms of an effective noise factor. The noise factor of an HTS filter with an insertion loss $1/G_1$ ($G_1 \leq 1$), operating at a temperature T relative to room temperature T_o, is [5]

$$F_1 = 1 + \frac{1 - G_1}{G_1}\left(\frac{T}{T_o}\right). \tag{1}$$

If the filter is cooled down close to the absolute zero temperature, $T \ll T_o$, no noise is added and $F_1 = 1$. For $G_1 = -0.5\,\mathrm{dB}$ and $T = 77\,\mathrm{K}$, the noise factor of the HTS-filter is $F_1 = 1.03$ (0.14 dB).

The total noise factor of the base-station receiver is obtained from the cascaded formula [5]

$$F_o = F_1 + \frac{F_2 - 1}{G_1} + \frac{F_3 - 1}{G_1 G_2}, \tag{2}$$

where F_1 is the noise factor of the HTS filter, F_2 is the noise factor of the LNA with a gain G_2, and F_3 is the noise factor of the rest of the receiver containing the downconverter and demodulator. With sufficient gain G_2, the contribution from F_3 is negligible and the noise factor of the receiver is determined by its front end. Here, as discussed, superconductivity brings in two great advantages: a low operating temperature and nearly lossless signal propagation in the pass band leading to an F_1 which is close to unit. The LNA adds only a small amount of noise and in practice we find that the effective operating noise figure is approximately $0.5\,\mathrm{dB}$ corresponding to $F_o = 1.12$.

When intermodulation distortion (IMD) due to the nonlinear character of the receiver is taken into account, the effective (generalized) noise factor F becomes:

$$F = F_o + \frac{N_{\mathrm{IMD}}}{N_{\mathrm{in}}}. \tag{3}$$

Here, $N_{\mathrm{in}} = kT_oW$ is the ambient noise power at the input, W is the channel bandwidth, and N_{IMD} is the IMD noise power referenced to the input of the receiver at a given frequency. Intermodulation distortion amplifies any fluctuations that are present in the interfering signals. The standard deviation σ_F of the effective noise factor can therefore be large. If the CDMA system cannot compensate for these fluctuations fast enough, they will have an adverse effect on the system capacity. Highly selective HTS filtering removes these fluctuations so that $\sigma_F \simeq 0$. Also, as discussed, the selectivity of the HTS filter is effective in reducing the out-of-band signal strength that leads to intermodulation distortion in the amplifier and the rest of the receiver following the filter. Thus, while $N_{\mathrm{IMD}}/N_{\mathrm{in}}$ can make a significant contribution to the effective noise factor when conventional filtering is used, the effective noise factor with HTS filtering is close to F_o.

III. Mean-Field CDMA

In this section, we consider the part of the IS-95A communication protocol between the mobile user and the base station that is responsible for transmission and reception of data [4], [6], [7], [9]. On the reverse link, this part of the CDMA system, the physical layer, is most affected by the improvements in the sensitivity and selectivity of the base-station receiver which is possible using high-temperature superconducting filters and cryocooled low-noise amplifiers.

A. Basic Theory

In a CDMA system, the bit error probability is a function of the ratio of energy per information bit E_b to noise spectral density N_o. Because a certain error probability is targeted, the bit energy-to-noise density ratio is fixed to $\zeta_v = (E_b/N_o)_{\mathrm{req}}$. Assuming perfect power control, each mobile user of n users per base-station cell adjusts its transmit power so that the received power level C_n at the base-station receiver fulfills the condition, $\zeta_v = (C/I)_n(W/R_v)$. Here I is the interference plus noise power, R_v is a given data rate, and W is the spread-spectrum bandwidth of the communication channel. The signals from the other $n-1$ users acts as additional noise and adds $\alpha_v(n-1)C_n$ to the background noise FN_{in}. Here, $\alpha_v \simeq 0.4$ is the average reverse-link voice activity factor, N_{in} is the background input noise power, and F is the receiver noise factor. Within a mean-field approximation, signals from other cells contribute $\alpha_v \xi n C_n$, with the reuse fraction $\xi \simeq 0.55$. Thus, the signal-to-interference plus noise ratio at the reveiver input is

$$\left(\frac{C}{I}\right)_n = \frac{C_n}{[(1+\xi)\,n - 1]\ \alpha_v\, C_n + FN_{\mathrm{in}}}. \tag{4}$$

For a given data rate R_v and spread-spectrum bandwidth W, the required signal-to-interference plus noise ratio is $(C/I)_n = \kappa_v$, where the normalized dimensionless data rate is

$$\kappa_v = \frac{\zeta_v R_v}{W}. \tag{5}$$

Setting this equal to $(C/I)_n$, given by Eq. (4), and solving for C_n gives

$$C_n = FN_{\mathrm{in}}\,\frac{K}{1-X}, \tag{6}$$

where $X = n/n_\infty$ is the cell loading. The constant K is

$$K = \frac{\kappa_v}{1 + \alpha_v \kappa_v} \tag{7}$$

and the pole capacity

$$n_\infty = \frac{1}{\alpha_v(1+\xi)K} \tag{8}$$

is the limiting theoretical cell capacity.

Although Eq. (6) is only an approximate mean-field result, it provides insight into the more detailed numerical simulations we will discuss later. In particular, it illustrates the interrelationship between coverage and capacity utilization in a CDMA system and the effect on these quantities of reducing the noise factor. First, one sees from Eq. (6) that, other quantities remain fixed, a reduction in the noise factor leads to a reduction in the handset power. In fact, this reduction can provide a direct measure of the change in the effective receiver noise factor F of a base-station when a superconducting filter system replaces the conventional front end.

B. Coverage Area

The coverage per base station is determined by the maximum allowed number of users per cell n_o, which defines the threshold of the cell loading as $X_o = n_o/n_\infty$. If the reverse-link signal propagation is characterized by a power law exponent γ so that the path loss varies inversely with distance as $1/r^\gamma$, then it follows from Eq. (6) that there is a simple relation between the cell radius ℓ and the cell loading threshold:

$$\ell = \ell_o \left(\frac{1 - X_o}{F}\right)^{1/\gamma}. \tag{9}$$

Here ℓ_o is the limiting radius of a cell such that a mobile user transmitting from the cell edge would have the required signal-to-noise ratio if there were no other users and the noise factor of the receiver were unity. Thus the coverage and capacity increases that result from a reduction in the noise factor of the base-station receiver are linked. Either one or both can be improved, but the amount of improvement is constrained by Eq. (9). This shows that for a fixed cell loading X_o, decreasing the noise factor increases the cell radius while for a fixed radius, a decrease in the noise factor allows for an increase in cell loading. For a fixed noise factor, the radius of the cell decreases as the cell loading increases. This is the so-called cell breathing effect and further illustrates the interrelationship between coverage and capacity utilization for a CDMA system.

C. Capacity Utilization

Alternatively, for a fixed cell radius, the theoretical unused capacity relative to the pole capacity, $1 - X_o$, is proportional to F. If the noise factor changes from F to F', the relative change in the loading threshold, $\Delta X_o = X_o' - X_o$, is

$$\frac{\Delta X_o}{X_o} = -\frac{\Delta F}{F}\left(\frac{1 - X_o}{X_o}\right), \tag{10}$$

where $\Delta F = F' - F$ is the change in the noise factor. It quantifies the enhanced capacity utilization. This is one of the most important mean-field results and is plotted in Fig. 1. The expression is universal in the sense that it only depends on the cell loading and noise factors. We see from Eq. (10) that if the network operates close to the maximum loading $X_o \sim 1$, a decrease in the noise factor has little effect on the cell loading. In contrast, if the loading is low, a decrease in the noise factor will lead to a noticeable increase in capacity utilization. For example, if $X_o = 0.5$ and the noise factor is lowered by a factor of 2 (3 dB), the loading can increase by $50\,\%$.

D. Coverage Efficiency

If the reverse-link is the limiting factor and the loading threshold X_o is fixed, then the average number of base-stations will vary as $F^{2/\gamma}$. Thus, lowering the noise factor while keeping the number of users per cell the same increases the coverage efficiency in terms of the coverage area per cell.

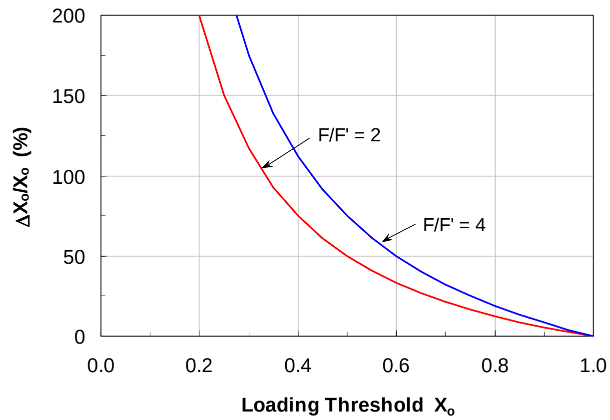

Fig. 1. The relative increase in the CDMA loading threshold X_o as a function of X_o, when the noise factor is decreased by a factor of 2 (3 dB) and 4 (6 dB).

The above scenario is well suited for situations where the number of users per cell can be fixed. However, often the limiting factor is the traffic density and we must consider whether the number of base stations can be reduced while still serving the same number of users per unit area. For a region of area S with $\mathcal{M}$ users per unit area, the number of base stations is

$$N_{BS} = \frac{S}{\pi \ell^2}, \tag{11}$$

where ℓ is the cell radius. Using the expression for ℓ from Eq. (9), this becomes

$$N_{BS} = \frac{S}{\pi \ell_o^2}\left(\frac{F}{1 - X_o}\right)^{2/\gamma}. \tag{12}$$

Here $S/\pi\ell_o^2$ is the minimum number of base stations one could have if $F = 1$ and $X_o = 0$. The number of base stations is determined by the requirement that the network can accommodate the traffic of $N = \mathcal{M}S$ users. Since the number of users per cell is $X_o n_\infty$, this requirement becomes

$$N = X_o n_\infty N_{BS}. \tag{13}$$

Substituting the expression in Eq. (12) for N_{BS}, we obtain an implicit equation for the cell loading X_o:

$$N = n_\infty \left(\frac{S}{\pi \ell_o^2}\right) X_o \left(\frac{F}{1 - X_o}\right)^{2/\gamma}. \tag{14}$$

Here the scale for the number of base stations is set by $S/\pi\ell_o^2$ and the scale for the carried number of users is set by $n_\infty S/\pi\ell_o^2$. Because ℓ_o and n_∞ both depend upon specifics of the network, it is convenient in the following to work with normalized quantities so that $\mathcal{N}_{BS} = N_{BS}/(S/\pi\ell_o^2)$ measures the number of base stations relative to $S/\pi\ell_o^2$ and $\mathcal{N} = N/(n_\infty S/\pi\ell_o^2)$ measures the number of users relative to $n_\infty(S/\pi\ell_o^2)$. Thus, $\mathcal{N} = X_o\mathcal{N}_{BS}$.

The cell loading X_o is determined from Eq. (14) for a given number of users $\mathcal{N}$. While this can be done for any

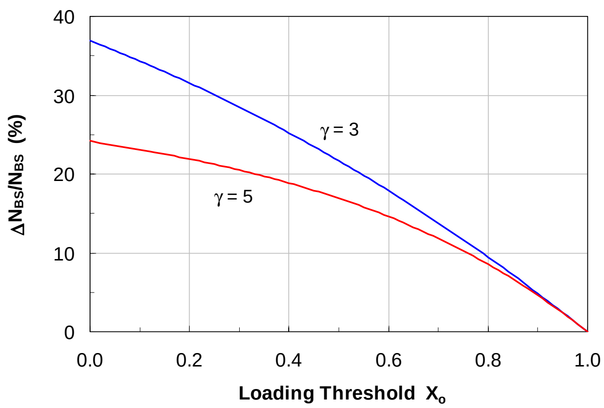

Fig. 2. Shown is the relative decrease in the number of base stations as a function of loading threshold X_o, when the noise factor is decreased by a factor of 2 (3 dB) for the propagation exponent $\gamma = 3$ and 5.

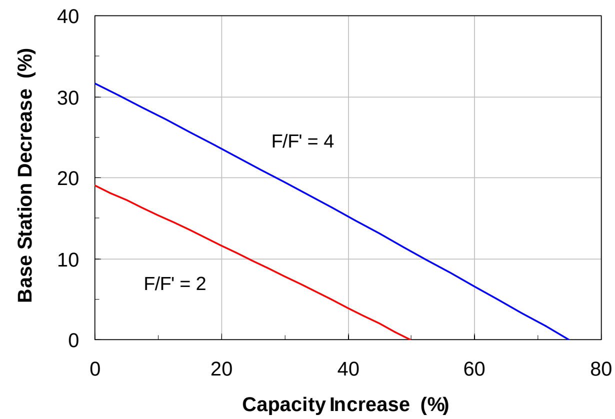

Fig. 3. The relative decrease in the number of base stations as a function of the capacity increase, when the noise factor is decreased by a factor of 2 and 4, for $X_o = 0.5$ (without HTS) and $\gamma = 4$.

propagation exponent, consider $\gamma = 4$ as an example. In this case, solving Eq. (14) for X_o, we obtain

$$X_o = \frac{\mathcal{N}^2}{2F}\left(\sqrt{1+\frac{4F}{\mathcal{N}^2}}-1\right) \tag{15}$$

and the number of required base stations becomes

$$\mathcal{N}_{BS} = \left(\frac{2F}{\mathcal{N}}\right)\frac{1}{\sqrt{1+\frac{4F}{\mathcal{N}^2}}-1}. \tag{16}$$

Note that the coverage efficiency is inversely proportional to $\mathcal{N}_{BS}$. Clearly, the coverage efficiency increases as the noise factor decreases. These equations are derived under the constraint that, for a given user density, the number of base stations is minimized. Varying the user density $\mathcal{M}$, and therefore $\mathcal{N}$, the impact of the noise factor F on the size of the network can be found for various situations.

(i) For a small user density, $\mathcal{N} \ll \sqrt{F}$, the cell loading becomes $X_o = \mathcal{N}/\sqrt{F}$, and the number of base stations is proportional to the square root of the noise factor:

$$\mathcal{N}_{BS} = \sqrt{F}. \tag{17}$$

Thus, when the user density is small, we get the same result independent of whether the number of users per base station or per unit area is kept constant. In this case, if the noise factor is reduced by a certain factor, the number of required base stations decreases by the square root of the same factor.

(ii) For a large user density, $\mathcal{N} \gg \sqrt{F}$, the cell loading is $X_o = 1 - F/\mathcal{N}^2$ and X_o approaches 1. In this limit, the number of base stations depends only weakly on the noise factor:

$$\mathcal{N}_{BS} = \mathcal{N}\left(1+\frac{F}{\mathcal{N}^2}\right). \tag{18}$$

In this case, the cell loading is so close to one that the interference due to the users dominates over the ambient noise, rendering the noise factor of the receiver irrelevant.

For example, if the propagation constant $\gamma = 4$ and F were decreased by a factor of 2, one would need only $1/\sqrt{2}$ as many base stations (of order 30 % fewer than without the superconducting front end) in the lightly populated regions. Fig. 2 illustrates the results more generally for γ equal to 3 and 5. As expected, the reduction in the number of base stations due to the reduced noise factor vanishes as the cell loading approaches one.

New network deployments can take an advantage of HTS improvements by trading off capacity utilization and coverage efficiency benefits. This will result in a cost-effective and better balance between deployment scenarios and network performance. Fig. 3 illustrates the optimal tradeoffs between the capacity increase and the coverage efficiency increase for a given noise-factor reduction. This reduces to the previous results outlined in Figs. 1 and 2 when either benefit vanishes.

IV. Fluctuations

In practice, imperfect power control will result in fluctuating received power at the base-station receiver. Because a CDMA cellular system is interference limited, it does not have a fixed number of channels as this depends on the amount of interference and the desired quality of service. The statistical nature of available links makes it convenient to define the capacity of the system in terms of a blocking probability. This is the probability that a new user will be denied access to the network. The number of users that can be supported for a given blocking probability is defined to be the soft, or Erlang, capacity of the system. The blocking probability is also known as the grade of service. In the following, we consider IS-95 CDMA.

Arriving calls are blocked, if the total amount of interference at a base-station receiver exceeds a certain value, as specified by the cell loading threshold X_o. The total amount of interference is

$$I = \sum_i \alpha_i C_i + F N_{\text{in}}, \tag{19}$$

where the sum is over all mobile users in the network, including the neighboring cells, and all users have the same average voice activity factor, $\alpha_v = \langle \alpha_i \rangle$. In general, propagation measurements show that the received carrier power for the ith user is a lognormal random variable [7]. Similarly, bit energy-to-noise spectral density is assumed to be a lognormal random variable,

$$\left(\frac{E_b}{N_o}\right)_i = \left\langle\frac{E_b}{N_o}\right\rangle_i e^{\sigma_o z_i}. \tag{20}$$

Here $\langle E_b/N_o\rangle_i$ is the median bit energy-to-noise spectral density value for the ith mobile user, σ_o is the standard deviation, and z_i is a random Gaussian variable with zero mean and unit standard deviation.

A new call is blocked when $I > I_o$. Here $I_o = F_o N_{\rm in}/(1-X_o)$ is the value for the total interference for a network with a desired quality of service set by the noise factor F_o and the loading threshold X_o. Thus, the blocking probability is

$$B = {\rm Prob}(I > I_o). \tag{21}$$

Defining $F = F_o(1+f)$ where f takes into account the IMD noise $N_{\rm IMD}$ arising from the nonlinear contribution in Eq. (3), the blocking condition can be written as $\sum_i \alpha_i C_i/I > X_o(f)$, where $X_o(f) = X_o - (1-X_o)f$. It can be shown [6], [7], [9] that, in Gaussian approximation with a Poisson distributed call traffic, the blocking probability is

$$B(X;f) = \frac{1}{2}{\rm Erfc}\left(\frac{X_o(f) - Xe^{\sigma_o^2/2}}{\sqrt{2\beta_o X}}\right). \tag{22}$$

Here, $X = A/n_\infty$ is the average cell loading and A is the average carried traffic per cell. The carried traffic A defines the soft (Erlang) capacity of the system per cell for a given blocking probability. The parameter β_o is defined as

$$\beta_o = \frac{\langle\alpha^2\rangle(1+\xi')}{\langle\alpha\rangle^2(1+\xi)^2 n_\infty}e^{2\sigma_o^2}. \tag{23}$$

Typical values of ξ and ξ' are 0.55 and 0.086, respectively [7].

For a constant effective noise factor, the blocking probability is given by Eq. (22) with $f = 0$. However, the blocking probability increases if the effective noise factor fluctuates, which would be the case when the base-station receiver does not have selective enough filtering. This reduces the capacity of the CDMA system. Let $p(f)$ be the probability distribution function of f. Then the blocking probability becomes

$$B(X) = \int_{-\infty}^{\infty} df\, p(f) B(X;f). \tag{24}$$

If the time scale of noise-factor fluctuations is much shorter than that of the power control, the power-control accuracy decreases and σ_o in Eqs. (22) and (23) must be replaced by the actual power control accuracy $\sigma > \sigma_o$. In general, $B(X)$ can be evaluated exactly by numerical integration. However, if f is a Gaussian random process, a closed-form result can be derived. Assuming that f is a Gaussian random variable with zero mean and standard deviation σ_F, the blocking probability is

$$B(X) = \frac{1}{2}{\rm Erfc}\left(\frac{X_o - Xe^{\sigma_o^2/2}}{\sqrt{2(\beta_o+\beta_F)X}}\right), \tag{25}$$

where $\beta_F = \sigma_F^2(1-X_o)^2/X$. For $\sigma_F < \sqrt{\beta_o X}/(1-X_o)$, the blocking probability is only weakly affected by a fluctuating effective noise factor. In contrast, outside this regime, the blocking probability increases rapidly with increasing σ_F. Note that β_F decreases as X_o increases. In intermodulation-distortion limited environments, poor filtering can be detrimental in terms of network capacity and lends further support to selective HTS filters. This behavior is demonstrated in Fig. 4, for $X_o = 0.5$ and 0.75.

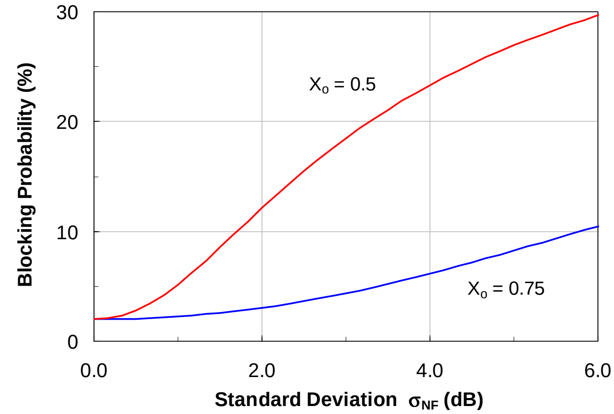

Fig. 4. The blocking probability $B(X)$ as a function of standard deviation $\sigma_{NF} = 10\sigma_F/\ln 10$, for $X_o = 0.5$ and 0.75. The offered traffic A_o is kept constant while the carried traffic $A = Xn_\infty$ is solved from the self-consistency condition, $A = A_o[1-B(X)]$. The offered traffic is determined so that, for $\sigma_F = 0$, the blocking probability $B = 2\,\%$,. The other parameters are $\sigma_o = 1.5\,$dB, $\xi = 0.55$, $\xi' = 0.086$, $\langle\alpha\rangle = 0.4$, $\langle\alpha^2\rangle = 0.31$, and $\kappa_v = 5/128$.

Even though the CDMA system does not have a well-defined number of channels, it still features a phenomenon known as “trunking efficiency” in which the soft capacity X increases more than the increase in the loading threshold X_o would imply. This is a direct consequence of the law of large numbers where the magnitude of fluctuations in the total channel interference grows only as $\sqrt{X}$. The capacity can therefore be increased further, because the standard deviation of interference fluctuations is actually decreased in relative terms. Also, since the relative standard deviation of the traffic distribution decreases as the magnitude of the traffic increases, a higher cell loading can be supported for the same blocking probability. However, in a CDMA system, trunking efficiency would be observed even under deterministic traffic conditions. For a deterministic cell loading,

$$\beta_o = \frac{\langle\alpha^2\rangle(1+\xi')}{\langle\alpha\rangle^2(1+\xi)^2 n_\infty}e^{2\sigma_o^2}\left(1 - \frac{\langle\alpha\rangle^2}{\langle\alpha^2\rangle}e^{-\sigma_o^2}\right). \tag{26}$$

The parameter β_o would be zero only if all the standard deviations characterizing the communication channel, σ_o and $\sigma_\alpha = \sqrt{\langle\alpha^2\rangle - \langle\alpha\rangle^2}$, were zero.

Specifically, consider the soft-capacity increase when the receiver noise factor is reduced. For a given grade of service B ($\leq 50\,\%$), the soft capacity X is obtained from Eq. (25) as

$$X = e^{-\sigma_o^2/2}\left[X_o + 2\epsilon\left(1 - \sqrt{1 + \frac{X_o}{\epsilon} + \frac{\beta_F}{2\beta_o\epsilon}}\right)\right], \tag{27}$$

where $\epsilon = \frac{1}{2}q^2\beta_o e^{-\sigma_o^2/2}$ and q is defined so that $B = \frac{1}{2}{\rm Erfc}(q)$. The increase in the soft capacity exceeds that of the loading threshold when the ratio ϵ/X_o does not vanish. It

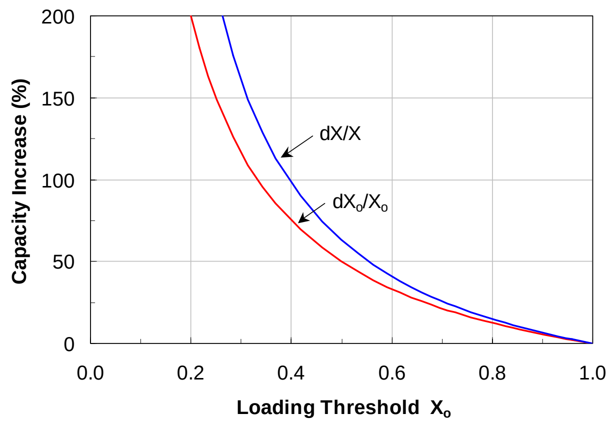

Fig. 5. The relative increase in the cell loading factor $\Delta X_o/X_o$ and the soft capacity $\Delta X/X$ as a function of the loading threshold X_o, when the noise factor is decreased by a factor of 2 (3 dB), $B = 2\,\%$, $\sigma_o = 1.5\,$dB, and $\sigma_F = 0$.

is illuminating to consider two limiting cases. For simplicity, let $\sigma_F = 0$.

First, for $X_o \gg \epsilon, \Delta X_o$, the relative increase in the soft capacity is

$$\frac{\Delta X}{X} = \left(1 + \sqrt{\frac{\epsilon}{X_o}}\right)\frac{\Delta X_o}{X_o}. \tag{28}$$

In the limit where $\epsilon/X_o \to 0$, the increase in the soft capacity is the same as the increase in the loading threshold. The increases are identical when the blocking probability $B = 50\,\%$, since $\epsilon = 0$.

Second, for $X_o, \Delta X_o \ll \epsilon$, the relative increase in the soft capacity is given by

$$\frac{\Delta X}{X} = 2\left(1 + \frac{\Delta X_o}{2X_o}\right)\frac{\Delta X_o}{X_o}. \tag{29}$$

Thus, the soft capacity is increased by more than a factor of two over the increase in the loading threshold. This case is relevant when the blocking probability is negligible.

For a typical situation with $F/F' = 2$, $X_o = 0.5$, $B = 2\,\%$, and $\sigma_o = 1.5\,$dB, we obtain $\epsilon = 0.027$ and the soft-capacity increase determined from Eq. (27) is 63 %, which is 26 % more than that suggested by the increase in the loading threshold, Eq. (10). Figure 5 illustrates the contribution of trunking efficiency to the actual capacity increase.

V. Numerical Simulations

The CDMA network is an interference-limited system in which the overall system performance relies on balancing the forward and reverse links. For balanced networks, improvements in the reverse link performance should be met with similar improvements in the forward direction. These may include increasing the total transmitted power of the base stations as well as adjusting the soft handoffs.

In this section, the network optimization problem of IS-95 CDMA is studied using a numerical simulation [1] that takes into account the fact that the forward-link performance differs from that of the reverse link. These differences, caused by multiple-access interference and soft handoffs, lead to different pole capacities for the forward and reverse links.

A. Statistical Model of a CDMA Network

The forward link of IS-95 CDMA includes four different channel types: a continuously transmitted pilot which provides a reference for all users, a continuously transmitted sync channel for base-station identification and timing, paging channels for control information, and traffic channels for voice. The number of traffic channels per cell is assumed to be 62. Typical target E_b/N_o values for these channels are -15 dB for the pilot, 6 dB for the sync and paging channels, and 7 dB for the traffic channels — the corresponding processing gains are 1, 1024, 256, and 128, respectively [7]. The actual simulation involves only separate pilot and traffic channels, whereas the remaining channels are included in the pilot channel by an overhead factor. Assuming that there is one active paging channel per base station, this factor is 2 dB for the above parameter values. Thus, the pilot E_b/N_o value used in the simulations is -13 dB.

The simulation utilizes a traffic model where calls arrive randomly and uniformly within the cluster area according to a Poisson distribution with rate λ. Call holding times are exponentially distributed with a mean time $1/\mu$, where μ is the average departure rate. Thus, in a time interval Δt, the average number of arriving calls is $\lambda\Delta t$ and the average number of terminations is $\mu\Delta t$. The time interval Δt is selected so that on average one call arrives during it: $\lambda\Delta t = 1$. If the offered traffic is 60 and the average call duration 120 s, $\Delta t = 2\,$s. Because the mobiles adjust their transmit power once in a 1.25-ms interval, the system has enough time to equilibrate between arriving and terminated calls.

If there were no limitations set by the network, at equilibrium the average traffic A (number of users) carried by the network would equal the offered traffic: $A = A_o \equiv \lambda/\mu$. However, because arriving calls must be denied access to the network if resources are not available and calls would have to be dropped if a sufficient link cannot be maintained, the offered and carried traffic usually differ. At equilibrium,

$$A = A_o(1 - B)(1 - D), \tag{30}$$

where B is the probability to block an arriving call from the network and D is the probability that a call is dropped [8]. We can also write

$$A = A_o(1 - B_{\text{eff}}), \tag{31}$$

where the effective blocking probability B_{eff} is defined in terms of the blocking probability B and the dropped-call probability D as

$$B_{\text{eff}} = B + (1 - B)D. \tag{32}$$

The effective blocking probability can also be interpreted as a metric for the quality of service where a smaller value of B_{eff} implies better quality of service.

A base station blocks a new call when there is no channel element available. This form of blocking is called hard blocking [9]. The number of links available for calls depends on the total amount of noise and interference. When the total amount of noise and interference at the input of a base-station receiver exceeds a threshold value, which is set to maintain the desired coverage and dropped-call rate, arriving calls are denied access to the network. This is soft blocking. It also accounts for mobile users that cannot access the network because a sufficient reverse or forward transmit power to make a connection is not available. An increase in the carried traffic for a given blocking probability indicates increased capacity, whereas a decrease in the blocking probability for a given carried traffic load implies a better grade of service.

A user is denied access to the network, if the cell loading is above the loading threshold X_o or if there are no traffic channels available. Each base station determines the cell loading X independently by comparing the user-induced interference to the ambient noise $FN_{\rm in}$. The capacity is defined in terms of the effective blocking probability $B_{\rm eff}$ that includes both hard and soft blocking: here, it is the number of users A_o (or A) for which the effective blocking probability equals 2 %.

In our numerical simulations, soft handoff provides macroscopic diversity where mobile users can simultaneously communicate with more than one base station. In the forward direction, the received signals from the different base stations are combined with maximal-ratio combining. In the reverse direction, however, selection combining is used where the received signal with the highest E_b/N_o value in the network is selected.

In the simulation, mobiles and base stations adjust their transmit power in finite steps. If the received E_b/N_o value is less than the target value, the transmit power is increased and vice verse. This procedure and the fact that the received power C_i is a lognormal random variable result in imperfect power control. For the chosen values used in the simulation, the standard deviation σ_o of the logarithm of the signal-to-total interference ratio, $\ln(C_i/I)$, measured at the base-station receiver, is 1.5 dB. A call is dropped, if the link reliability is less than 80 %, which happens when the received E_b/N_o is less than the target E_b/N_o value more than 20 % of the time due to reverse or forward transmit power limitations.

The voice activity is described by a quaternary random process that parallels the natural voice pattern. The probability of full rate transmission is 29.1 %, half rate is 3.9 %, 1/4 rate is 7.2 %, and 1/8 rate is 59.8 %. Thus, in the reverse link, the average voice activity factor is $\langle\alpha\rangle = 0.4$ and $\langle\alpha^2\rangle = 0.31$. In the forward link, the power-control bit is taken into account increasing $\langle\alpha\rangle$ to 0.45.

The simulation tool can employ any propagation model. As an illustration, we use the empirical CCIR formula, which is the Hata model for a medium-small city [10]. In the simulations shown below, the base-station antenna height is 50 m, the mobile antenna height is 2 m, the carrier frequency is 830 MHz, and 15 % of the study area is covered by buildings. While forward channels are transmitted orthogonally, multipath propagation usually leads to forward-link interference. Here we assume that 70 % of the transmitted power appears as interference.

B. CDMA Network Performance

As an example, we consider a cluster of three omnidirectional cells that is designed to cover an area of about 100 km^2. The base stations form an equilateral triangle which is 6 km on a side. The required coverage area of the network is fixed so that mobile users within 4 km from any base station should be served with good quality of servive. Setting the cell radius at approximately 4.3 km, the implied margin in the link budget is sufficient to keep the number of dropped calls small for most cases. The handset noise figure will be taken to be 8 dB and the handset peak power will be set at 200 mW, which corresponds to 23 dBm. The nominal base-station noise figure without the HTS front end will be taken to be 5 dB. The superconducting front end has the ability to decrease the base-station noise figure down to 2 dB. The capacity of the network is measured for a constant effective blocking probability of approximately 2 %. The data was collected over 50,000 time intervals [11].

Figures 6 and 7 summarize the simulation results. Without the HTS front end, limiting the loading threshold X_o to 0.5 allows the cluster to cover the desired area. The three-site cluster can handle an offered traffic of 54 users for the specified effective blocking probability. This corresponds to a soft capacity of 53 users (average carried traffic). The dropped-call probability D is 0.2 %. A sufficient forward-link coverage and soft capacity is obtained when the pilot power is 1 W and the available total base-station transmit power is 11 W.

With the HTS front end, the loading threshold X_o can now be increased to 0.75 while maintaining the same required coverage area. For $B_{\rm eff} = 2\,\%$, the offered traffic can be increased to $A_o = 93$ users. The average carried traffic A is 91 users and the dropped-call probability D is 0.3 %. The forward link does not limit the capacity of the cluster, if the pilot power is increased to 1.3 W and the maximum base-station transmit power to 25 W. Thus, a 3-dB reduction in the base-station receiver noise figure can yield a 75 % increase in the voice capacity for the given coverage area provided the pilot power is increased to 1.3 W and the base-station transmit power is increased to 25 W.

The "measured" probability distribution functions for the handset and base-station transmit powers are given in Fig. 6. If the base-station noise figure is reduced by 3 dB but the loading threshold X_o and the effective blocking probability $B_{\rm eff}$ are kept the same, the soft capacity of the network will remain the same. However, the number of dropped calls will vanish, and the probability distribution function of the handset transmit power will shift 3 dB to lower power levels, as shown in Fig. 6(a). The average handset transmit power in this simulation was also reduced 3 dB. Note that even if the loading threshold is also increased to facilitate the capacity increase, the probability distribution functions remain essentially the same as they were for the lower threshold without the HTS front end.

The shape of the probability distribution function for the handset transmit power shown in Fig. 6(a) can be understood by the fact that the transmit power cannot exceed the peak power of 23 dBm (200 mW). At low power levels, the probability distribution function is determined by the mobiles close to the base stations. The differential probability of having mobiles at a distance r from the base station is $dP \propto rdr$ in which case their transmit power in dBm units is $C = 10\lg r + const$. Thus, the probability distribution follows a curve that has the simple form: $dP/dC \propto 10^{C/(5\gamma)}$.

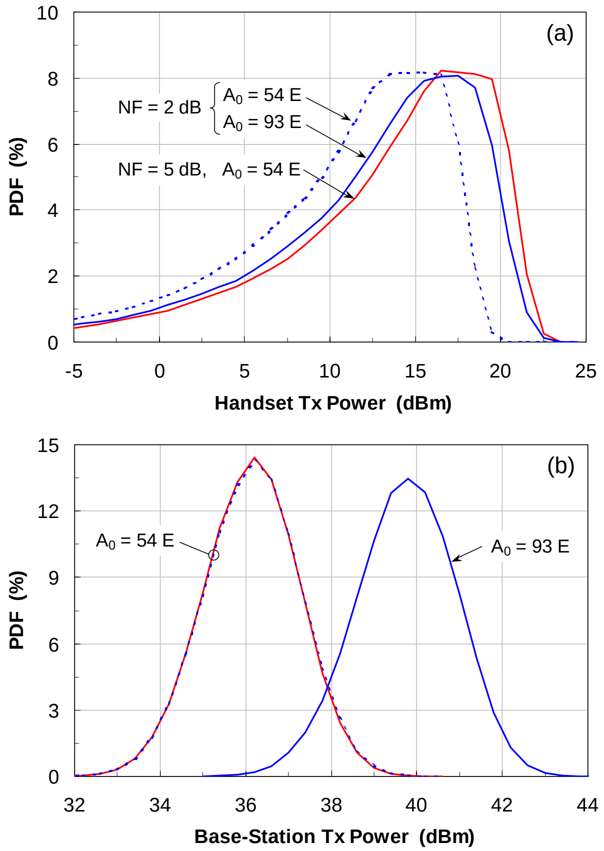

Fig. 6. The probability distribution function of (a) the handset transmit power and (b) the total base-station transmit power when the base-station receiver noise figure is 5 dB (red line) and 2 dB (blue line). Without the HTS front end ($NF = 5$ dB), the offered traffic A_o is 54 users, the reverse-link loading threshold X_o is 0.5, and the pilot power is 1 W. With the HTS front end ($NF = 2$ dB), the offered traffic A_o is 93, the reverse-link loading threshold X_o is 0.75, and the pilot power is 1.3 W. As a comparison, also shown is the probability distribution function (dashed blue line) for $F = 2$ dB, $A_o = 54$, $X_o = 0.5$, and a pilot power of 1 W.

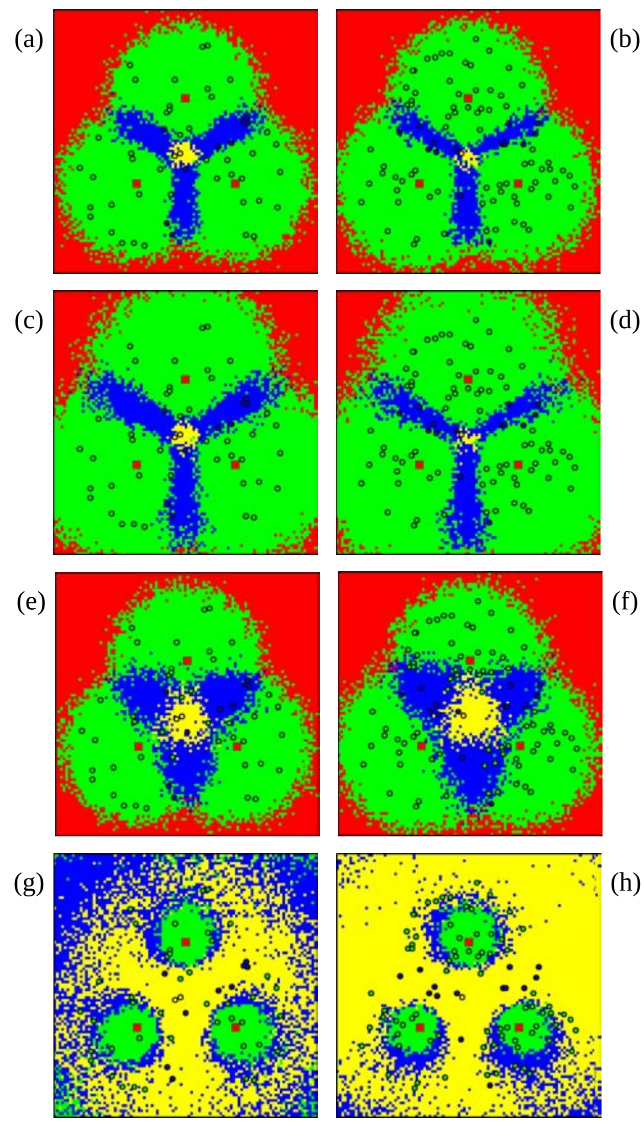

Fig. 7. The instantaneous coverage areas, indicating the appropriate soft handoff regions for adding a new user, when the base-station receiver noise figure NF is 5 dB and the number of mobile users is 53 (without HTS filters) and when NF is 2 dB and the number of mobile users is 91 (with HTS filters): the composite coverage area for (a) $NF = 5$ dB and (b) $NF = 2$ dB, the pilot coverage area for (c) $NF = 5$ dB and (d) $NF = 2$ dB, the reverse coverage area for (e) $NF = 5$ dB and (f) $NF = 2$ dB, the forward coverage area for (g) $NF = 5$ dB and (h) $NF = 2$ dB. Base stations are denoted by red squares and mobiles by filled circles with their color giving their soft handoff state. Red shows no coverage, green the one-way soft handoff region, blue the two-way soft handoff region, and yellow the three-way soft handoff region. The area shown is 16 km $\times$ 16 km and the distance between the base stations is 6 km. As noted in the text, in order for the forward link not to limit this increased capacity, the pilot power is increased from 1 to 1.3 W and the maximum base-station transmit power from 11 to 25 W when the HTS front end is used.

Figure 6(b) illustrates the probability distribution function for the base-station transmit power. Initially, the average base-station transmit power is 36.3 dBm (4.3 W) and the standard deviation is at 1.1 dB. With increased traffic loading, the average base-station transmit power is increased by 3.6 dB, while the standard deviation remains the same. Similarly, the peak transmit power increases 3.6 dB from 40.4 dBm (11 W) to 44 dBm (25 W). In order to manage the increased reverse-link capacity, the power-handling capabilities of the base stations must be increased by more than a factor of two to ensure that the forward link does not limit the system capacity. As long as the amount of traffic and the coverage area remain the same, reducing the receiver noise factor has no effect on the base-station transmit power. The probability distribution functions are broadened mainly because of variations in the number and location of mobile users.

Figure 7 shows the mobile user locations at one random instant of time with 53 and 91 users and the corresponding coverage areas. For the increased capacity, the reverse-link coverage area is the same, as are the pilot and composite ones. The forward-link coverage for traffic is larger for 91 users, because the base-station transmit power was increased so that the unevenly distributed loading conditions and large loadings can be handled without the forward link limiting the

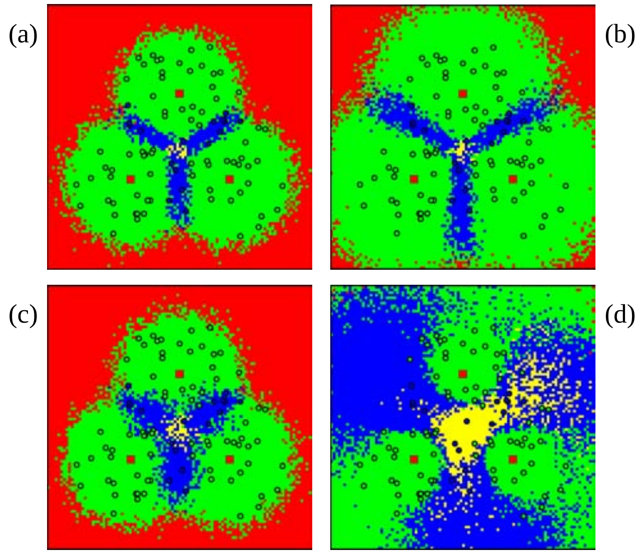

Fig. 8. The instantaneous coverage areas, indicating the appropriate soft handoff regions for adding a new user, when the base-station receiver noise figure NF is 5 dB and the number of mobile users is 91: (a) the composite coverage area, (b) the pilot coverage area, (c) the reverse coverage area, and (d) the forward coverage area. Base stations are denoted by red squares and mobiles by filled circles with their color giving their soft handoff state. Red shows no coverage, green the one-way soft handoff region, blue the two-way soft handoff region, and yellow the three-way soft handoff region. The area shown is 16 km $\times$ 16 km and the distance between the base stations is 6 km. The pilot power is 1 W and the maximum base-station transmit power 11 W.

capacity. Note the slightly reduced two- and three-way soft handoff regions in the composite and pilot plots.

The effect of cell breathing is illustrated in Fig. 8, which shows the coverage areas for the three-site cluster without the HTS front ends when there are 91 users present. Clearly, the reverse and forward coverage areas are smaller than those with the HTS front ends and 91 users, shown in Fig. 7. The pilot coverage area is less sensitive to the number of users with the exception that the two and three-way soft handoff regions have shrunk.

C. Network Planning and Capacity

The capacity utilization of the network is determined by the distance between base stations and the propagation loss. Frequently, the capacity utilization can be increased by sectorization and cell splitting. We have shown that reducing the system noise factor will lead to a similar result but that this improvement is sensitive to the cell loading that the network is designed for. Here the case is considered in which the location of base stations is constrained. Similar constrains may be imposed on the antenna height, forcing the network to have a particular loading threshold.

The capacity utilization of the cluster network and the capacity increase due to the HTS front end is strongly influenced by the loading threshold, which is a function of base-station antenna height. As the antenna height is increased, the propagation loss decreases allowing the use of larger loading thresholds; see Fig. 9. For a given loading threshold X_o and blocking probability, the average cell loading X and the concomitant capacity increase can be estimated analytically from Eq. (27) and also computed from the numerical simulation.

Main reasons for the deviation between numerical simulation and analytical results are soft handoff and blocked and dropped calls, which are more likely to occur when the number of users N in the network is high. It is particularly important to realize that blocked and dropped calls will reduce the probability of having high N values. In fact, numerically obtained probability distribution functions of N are approximately Gaussian distributed with a standard deviation less than $\sqrt{A}$, where $A = \langle N \rangle$ is the average value of N.

For the purposes of comparison of numerical simulation and analytical mean-field results, let N_k denote the instantaneous number of users in a soft handoff state with the kth cell's base station ($k = 1, \ldots, N_{BS}$). As a generalization, the instantaneous loading X_k of the kth cell is defined so that the instantaneous noise rise relative to average thermal noise floor, $\langle F \rangle N_{\rm in}$, at the kth base station is $(1 - X_k)^{-1}$. Further, assume that the number of users in soft handoff with the kth base station and its cell loading are linearly related,

$$X_k = \frac{N_k}{n_\infty}, \tag{33}$$

where the factor of proportionality n_∞ defines the pole capacity. It is convenient to write Eq. (33) in the form

$$\frac{1}{N_{BS}} \sum_{k=1}^{N_{BS}} X_k = \left(\frac{N}{N_{BS}} \right) \left(\frac{\eta}{n_\infty} \right). \tag{34}$$

The soft-handoff factor η measures the channel overhead due to soft handoff and is given by

$$\eta = \frac{1}{N} \sum_{k=1}^{N_{BS}} N_k. \tag{35}$$

For a wide range of values of carried traffic A, the ratio η/n_∞ is independent of N, and we can approximate

$$X \simeq \left(\frac{A}{N_{BS}} \right) \left\langle \frac{\eta}{n_\infty} \right\rangle. \tag{36}$$

Here, the average cell loading $X = \langle X_k \rangle$. In mean-field theory, the above definition of n_∞ reduces to Eq. (8), for $\eta = 1$.

We note in passing that random variables N, $1/n_\infty$, and η are approximately Gaussian distributed and exhibit a variable degree of cross-correlation. While η and $1/n_\infty$ are moderately negatively correlated with N, the ratio η/n_∞ shows only a small amount of correlation with N. Thus, for the considered three-site network, Eq. (36) is well obeyed with $\langle \eta/n_\infty \rangle^{-1}$ equal to 50.8. Furthermore, for $A_o = 54\,\mathrm{E}$, $\langle \eta \rangle = 1.24$ and $\langle 1/n_\infty \rangle^{-1} = 63.4$.

In contrast, the mean-field approach postulates a Poisson distributed traffic load and uses $\eta = 1$. If all arriving calls were admitted to the network and no calls were dropped, the numerically obtained traffic distribution would be Poisson distributed as well. However, the adopted call admission policy

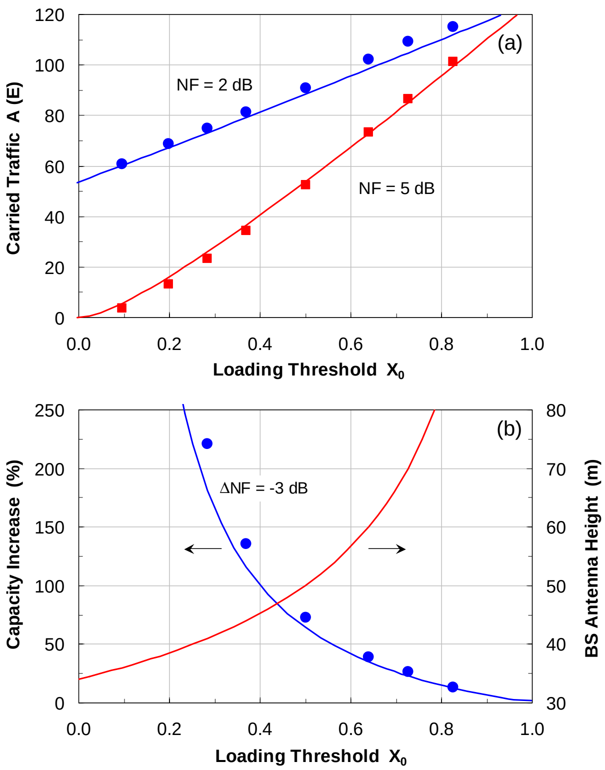

Fig. 9. (a) The average carried traffic A as a function of the loading threshold X_o for the base-station receiver noise figure $NF = 2\,\mathrm{dB}$ (blue circles) and 5 dB (red squares) and (b) the corresponding capacity increase, $\Delta X/X$, and the base-station antenna height as a function of X_o. Quantitative numerical values of X and $\Delta X/X$ are computed by simulation for $B_{\rm eff} = 2\,\%$ and their corresponding analytical values are obtained from Eq. (27) for $B = 2\%$, $\sigma_o = 1.5\,\mathrm{dB}$, $\xi = 0.095$, and $\xi' = 0.029$ [12]. Simulation results are denoted by symbols and analytical predictions by lines.

changes the carried traffic distribution to one that is better described as Gaussian with a standard deviation about 8 % smaller than $\sqrt{A}$. To account for the increased A due to the modified traffic distribution, we increase the analytical pole capacity 9 %. Thus, in the analytical mean-field theory, $n_\infty = 63.4$, for $\xi = 0.095$. This correction does not affect the capacity increase estimates.

The numerical and analytical results on the capacity increase due to the HTS front end are in good agreement, adding confidence to our conclusions. At high loading threshold values X_o, the simulation predicts a smaller capacity increase because of the increased forward multi-user interference and because the carried traffic is large enough for hard blocking to occur more often. These effects are also neglected in the analytical treatment.

D. Effect of IMD Noise on Network Properties

We conclude this section by examining the effect of IMD noise on the blocking and dropped-call probabilities. We assume that the noise factor of the base-station receiver is a lognormal random process:

$$F = F_o e^{\sigma_F x}, \tag{37}$$

where x is a Gaussian random process with zero mean and unit standard deviation [13]. The mean and standard deviation of the noise figure, $NF = 10 \lg F$, are $\langle NF \rangle = 10 \lg F_o$ and $\sigma_{NF} = 10\sigma_F / \ln 10$.

Two limiting scenarios are concidered where the time scale of x is either slow or fast relative to the reverse-link power control. In the former case, the system follows adiabatically the noise-factor fluctuations so that the network always maintains an equilibrium state. While the quality of service, as measured by the link quality, is not affected by slow noise-factor fluctuations, the probability of dropped calls can increase drastically, because all mobile users associated with a given base station are collectively affected by these fluctuations resulting in occasional large coverage holes. In the latter case, noise-factor fluctuations are too fast for the power control to follow. This causes an additional broadening of the reverse-link E_b/N_o, because mobile users effectively follow the average value of C/I due to slow power control. In order to maintain the same level of quality of service, the target value of E_b/N_o must be increased when the network is exposed to fast IMD fluctuations.

First, consider an isolated omnidirectional cell serving randomly distributed mobile users in close proximity to the base station so that the link reliability is not limited by the maximum handset transmit power. Thus, in this scenario, there are no dropped calls. As an initial design principle, the offered traffic is chosen so that the blocking probability is 2 % when there is no IMD noise, yielding $A_o = 21\,\mathrm{E}$. In the presence of IMD noise, the blocking probability is calculated by numerical simulation and from Eq. (24) for a cell loading X such that

$$A = A_o \left[1 - B(X)\right], \tag{38}$$

where the carried traffic is $A = X n_\infty$. Numerically and analytically obtained blocking probabilities are compared in Fig. 10(a), which shows a good agreement both for slow and fast IMD fluctuations. As the standard deviation of IMD noise increases, the probability of blocking a new call increases rapidly reducing the capacity of a cell.

Fig. 10(b) shows both the analytically and numerically calculated power-control accuracies, which are defined as the standard deviation of the reverse-link E_b/N_o. While slow IMD fluctuations have no effect on the accuracy of power control, fast IMD fluctuations reduce the accuracy because of the time scale difference. The effect of fast IMD fluctuations on the power-control accuracy can be estimated by noting that the standard variance of E_b/N_o is a sum of the intrinsic variance σ_o^2 and the standard variance σ_I^2 of the total interference, Eq. (19):

$$\sigma^2 = \sigma_o^2 + \sigma_I^2. \tag{39}$$

For $A \gg 1$, σ_I is same as the standard deviation of the interference variable,

$$z_I = \ln \left[X e^{\sigma_o^2/2} + (1-X) e^{\sigma_F x} \right]. \tag{40}$$

where the multi-user interference is replaced by its average value. For $\sigma_F < 1$ ($\sigma_{NF} < 4\,\mathrm{dB}$), an asymptotic estimate for

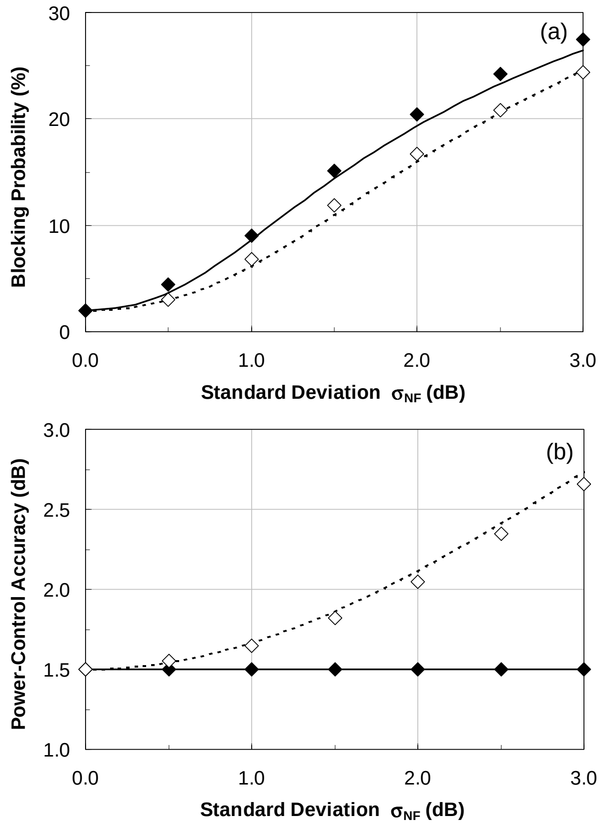

Fig. 10. (a) The blocking probability and (b) the reverse power-control accuracy, as measured by the standard deviation of the received E_b/N_o, as a function of the standard deviation σ_{NF} of the IMD noise for one isolated omnidirectional cell. The propagation loss is given by the CCIR model, the offered traffic is $A_o = 21\,\mathrm{E}$, the loading threshold $X_o = 0.5$, the average base-station receiver noise figure $\langle \sigma_{NF} \rangle = 5\,\mathrm{dB}$, and $\sigma_o = 1.5\,\mathrm{dB}$. Simulation and analytical results for slow IMD fluctuations are shown by filled diamonds and the black line and for fast IMD fluctuations by open diamonds and the dashed line.

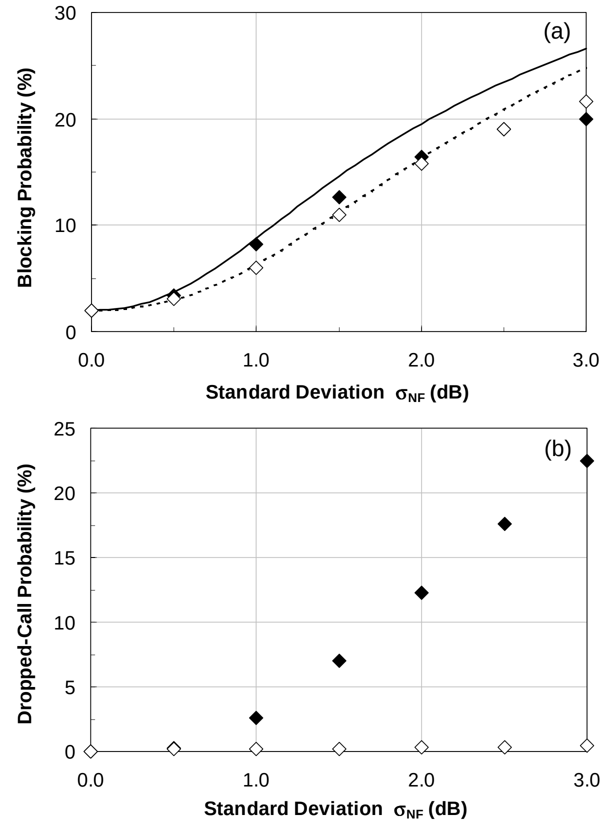

Fig. 11. (a) The blocking probability and (b) the dropped-call probability as a function of the standard deviation σ_{NF} of the IMD noise for a network with three omnidirectional cells. The propagation loss is given by the CCIR model, the offered traffic is $A_o = 54\,\mathrm{E}$, the loading threshold $X_o = 0.5$, the average base-station receiver noise figure $\langle NF \rangle = 5\,\mathrm{dB}$, $\sigma_o = 1.5\,\mathrm{dB}$, $\xi = 0.095$, and $\xi' = 0.029$. Simulation and analytical results for slow IMD fluctuations are shown by filled diamonds and the black line and for fast IMD fluctuations by open diamonds and the dashed line.

σ_I can be derived where

$$\sigma_I = \sigma_F \left(1 + \frac{X}{1-X} e^{\sigma_o^2/2}\right)^{-1}. \qquad (41)$$

This formula is also exact for any σ_F, when $X = 0$ or 1. Thus, as the time scale of IMD fluctuations shortens, the standard deviation of E_b/N_o *increases* and the accuracy of power control decreases.

With IMD fluctuations, the probability distribution of received power levels C at a base-station receiver is also lognormal. In contrast to the reverse-link E_b/N_o, however, the standard deviation of $\ln(C/N_{\mathrm{in}})$ *decreases* when the time scale of IMD fluctuations shortens. For slow IMD fluctuations, the standard deviation of $\ln(C/N_{\mathrm{in}})$ is $\sqrt{\sigma_o^2 + \sigma_F^2}$. For fast IMD fluctuations, C is decoupled from the instantaneous noise factor and depends only on its average value. Therefore, the standard deviation of $\ln(C/N_{\mathrm{in}})$ is reduced approximately to σ_o. This phenomenon where the fluctuations in the received power levels is reduced to its intrinsic value in the limit of fast IMD fluctuations is similar to "motional narrowing" observed in many physical systems where external fluctuations are too fast for a system under consideration to follow [14].

Next, the three-site cluster previously introduced in Section V.B. is exposed to IMD noise, described by Eq. (37). The results are summarized in Fig. 11 for a reverse-link call admission policy with $X_o = 0.5$ and for $A_o = 54\,\mathrm{E}$. Even with multiple cells and soft handoff, the numerical and analytical blocking probabilities are in fair agreement. Slow IMD fluctuations cause the main deviation in the blocking probability through the increased number of dropped calls, because the network is designed for a particular user distribution and capacity assuming that no IMD noise exists. The network is less sensitive to fast IMD fluctuations, as demonstrated by the low dropped-call probability; see Fig. 11(b).

Finally, assume that no call admission policy on the reverse link has been implemented by setting $X_o = 1$. This scenario is frequently encountered in practice where networks base their admission of arriving calls only on the availability of forward-link resources. We further assume that the standard deviation of IMD noise is fixed to $\sigma_{NF} = 2.2\,\mathrm{dB}$ but that the offered traffic is varied. We consider three types of networks: ones whose base-station receivers are exposed to IMD noise and have $NF = 5\,\mathrm{dB}$, those ones with receivers that are able to

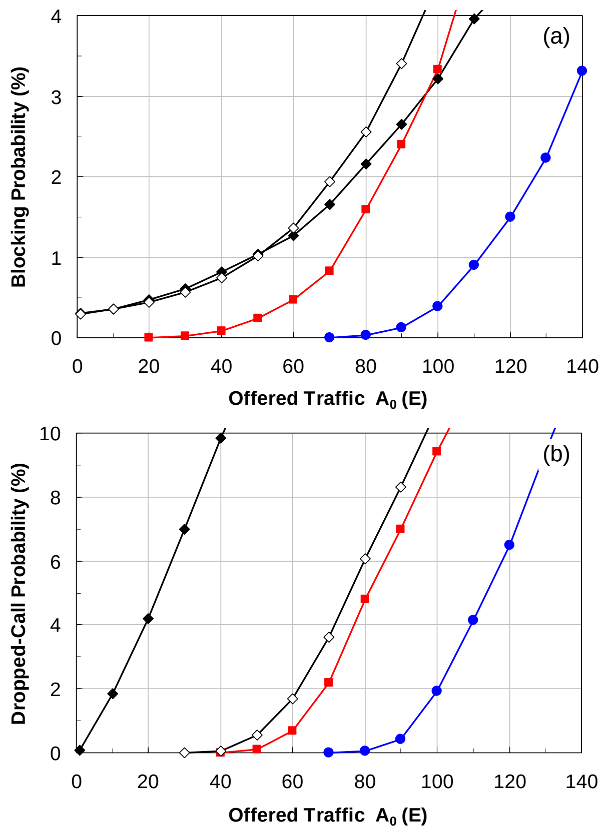

Fig. 12. (a) The blocking probability and (b) the dropped-call probability as a function of the offered traffic A_o for a network with three omnidirectional cells. The propagation loss is given by the CCIR model, the loading threshold $X_o = 1$, and $\sigma_o = 1.5\,\text{dB}$. Shown are simulation results for slow IMD fluctuations with $\langle NF \rangle = 5\,\text{dB}$ and $\sigma_{NF} = 2\,\text{dB}$ (black diamonds), for fast IMD fluctuations with $\langle NF \rangle = 5\,\text{dB}$ and $\sigma_{NF} = 2\,\text{dB}$ (open diamonds), for $\langle NF \rangle = 5\,\text{dB}$ and $\sigma_{NF} = 0$ (red squares), and for $\langle NF \rangle = 2\,\text{dB}$ and $\sigma_{NF} = 0$ (blue circles).

eliminate IMD noise but still have $NF = 5\,\text{dB}$, and lastly ones whose receivers are so selective and sensitive that the IMD noise is absent and $NF = 2\,\text{dB}$. As Fig. 12 demonstrates, the capacity and the quality of service of the network are improved by both eliminating the IMD noise and reducing the noise figure 3 dB.

Either the blocking probability or the dropped-call probability can be used to define the network capacity. The effective blocking probability, Eq. (32), is a particularly weighted measure of the quality of service and is suitable for this purpose. Ideally, in networks that use well-defined call admission policies to maintain an adequate quality of service, calls are dropped only rarely and the blocking probability is used to define the capacity of a network. Here, however, existing calls are being dropped before the blocking probability starts to increase, and the effective blocking probability is approximately same as the dropped-call probability. Note that mobile users unable to connect to the network because of either insufficient reverse or forward transmit power are accounted as blocked calls.

Defining the capacity as the offered traffic for which the

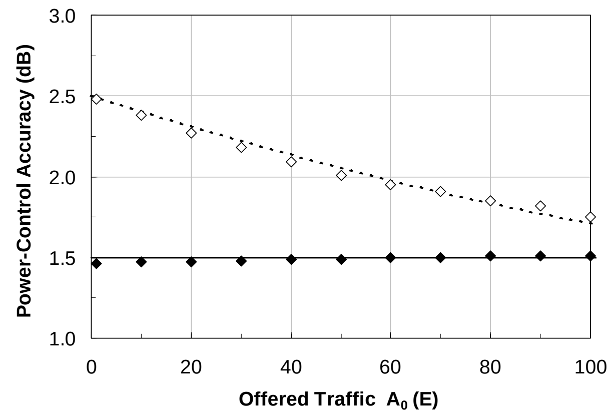

Fig. 13. The reverse power-control accuracy, as measured by the standard deviation of the received E_b/N_o, as a function of the offered traffic A_o for a network with three omnidirectional cells. The propagation loss is given by the CCIR model, the loading threshold $X_o = 1$, the average base-station receiver noise figure $\langle NF \rangle = 5\,\text{dB}$, $\sigma_{NF} = 2\,\text{dB}$, and $\sigma_o = 1.5\,\text{dB}$. Simulation and analytical results for slow IMD fluctuations are shown by filled diamonds and the black line and for fast IMD fluctuations by open diamonds and the dashed line.

dropped-call probability is $2\,\%$, we can conclude from Fig. 12 that, in this particular example, the capacity of the network utilizing sensitive and selective base-station receivers characterized by $NF = 2\,\text{dB}$ and $\sigma_{NF} = 0$ is 105 E. In the presence of IMD noise the capacity is only 15 to 42 E, depending on the time scale of IMD fluctuations. The capacity increase due to selectivity and sensitivity ranges from $150\,\%$ to $600\,\%$. If the receiver is only selective but not sensitive so that $NF = 5\,\text{dB}$ and $\sigma_{NF} = 0$, the capacity of the network is 73 E. This corresponds to a $74\,\%$ to $390\,\%$ increase in the capacity relative to the nonselective base-station receivers in the presence of IMD noise. In the absent of IMD noise, a 3-dB decrease in the base-station noise figure will approximately increase the capacity utilization by $44\,\%$.

An interesting aspect of the three-cell network analyzed in Fig. 12 is that the effect of IMD noise on the accuracy of reverse-link power control is obtained using Eqs. (39) and (41). As is apparent in Fig. 13, the analytical theory quantitatively explains the numerical simulation results for slow and fast IMD noise fluctuations. Thus, the adverse impact of imperfect power control on the quality of service and the capacity utilization can be determined.

We conclude this section by noting that because the reverse link of certain third generation systems is conceptually similar to that of IS-95, our findings should apply to these systems as well. The accuracy of power control in the presence of IMD noise is one relevant example with important implications for any spread-spectrum system.

VI. CDMA2000

In this section, we extend our analysis to discuss CDMA2000 modes of IS-2000 and IS-856. We begin with a brief review of the features of the CDMA2000 protocol that enter in determining the effects of an HTS front end on network performance.

Third generation wireless communications aim towards increased data rates and a wide variety of services [15]. As an evolutionary implementation of current IS-95 air interface technology, CDMA2000 is designed to provide data rates that meet the IMT-2000 performance requirements of at least 144 kb/s in a vehicular environment, 384 kb/s in a pedestrian environment, and 2.048 Mb/s in an indoor office environment.

The CDMA2000 air interface has two interoperable modes that are optimized either for voice and medium data speeds or for high speed data and internet access. The first mode of operation has two phases. Phase one, known as IS-2000 1xRTT, enables 144 kb/s packet data in a mobile environment and is based on existing spectrum allocations with 1.25 MHz carriers. Phase two (3xRTT) will initially support a 5 MHz channel bandwidth with a chip rate of 3.6864 Mc/s.

The second mode of CDMA2000, known as 1xEV, is based on the evolution of the 1xRTT air interference standard and is designed for high-rate packet data. It compromises two phases utilizing channels of 1.25 MHz wide. Phase one (1xEV-DO), specified in IS-856, offers packed-data-only service capable of transmitting at a data rate that varies from 38.4 kb/s to 2.4576 Mb/s in the forward link and from 9.6 kb/s to 153.6 kb/s in the reverse link. Phase two (1xEV-DV) supports mixed voice and data and is currently under development.

A. 1xRTT

Here, we consider the reverse link of IS-2000 1xRTT [16], [17]. Specifically, the reverse link is assumed to support a pilot channel and a traffic channel. The reverse traffic channel may be mapped to a fundamental channel for voice (data rate R_v) or to a variable-rate supplemental channel for data (data rate R_d) depending on the application requested by the user. Multipath propagation in time dispersive radio environments leads to co-channel interference even within the same cell: multipaths from the same source interfere with each other. Assuming a maximal ratio combining of paths with equal power fractions, the total interference for n voice users and m data users per cell is

$$I = (1+\xi)[n(\alpha_{pv}c_{pv} + \alpha_d c_v) + m(\alpha_{pd}c_{pd} + \alpha_d c_d)] + FN_{\text{in}}. \tag{42}$$

Here c_{pv}, c_{pd}, c_v, and c_d are the received power levels for the pilot, fundamental, and supplemental channels, respectively. If a gated mode of operation is selected where certain power control groups are periodically gated off [17], [18], the transmit duty cycle can be less than 100 % and α's are the activity factors of their respective channels. If the transmit duty cycle is 100 % but the gain factor of each channel is varied [17], α's are the mean gain values characteristic to the particular service ($0 \leq \alpha_k \leq 1$). Because our conclusions are independent of the particular mode of operation, without loss of generality, the gated mode is considered in the following, and the pilot and traffic channels are assumed to have the same transmission duty cycles: $\alpha_{pv} = \alpha_v$ and $\alpha_{pd} = \alpha_d$.

While the utilization of the reverse link is application dependent, for the World Wide Web and Electronic Mail, the data activity factor α_d is estimated to be small [19]. Given distinct target E_b/N_o values for all four channels, four equations are obtained:

$$\kappa_k = \frac{c_k}{I}, \qquad (k = pv, pd, v, d) \tag{43}$$

where the normalized dimensionless data rates are

$$\kappa_k = \frac{\zeta_k R_k}{W}, \qquad (k = pv, pd, v, d) \tag{44}$$

and $R_{pv}, R_{pd} = W$. Solving these equations for c_k, we obtain

$$c_k = FN_{\text{in}} \frac{\kappa_k}{1-X}, \qquad (k = pv, pd, v, d) \tag{45}$$

where the cell loading factor is generalized to

$$X = \frac{n}{n_\infty} + \frac{m}{m_\infty}. \tag{46}$$

Here, the pole capacities for the voice and the data have the form

$$n_\infty = \frac{1}{\alpha_v(1+\xi)K_v}, \tag{47a}$$

$$m_\infty = \frac{1}{\alpha_d(1+\xi)K_d}, \tag{47b}$$

where $K_v = \kappa_v + \kappa_{pv}$ and $K_d = \kappa_d + \kappa_{pd}$. The users must therefore transmit so that the received power, $C_k \equiv c_{pk} + c_k$ ($k = v, d$), at the base-station receiver for each voice ($k = v$) and data ($k = d$) user is

$$C_v = FN_{\text{in}} \frac{K_v}{1-X}, \tag{48a}$$

$$C_d = FN_{\text{in}} \frac{K_d}{1-X}. \tag{48b}$$

These formulas form the basis for the subsequent analysis.

In general, coherent detection of voice and data lowers the required bit energy-to-noise spectral density by about 3 dB for the same bit error rate [7]. As data rates increase, additional improvements in the performance are possible due to more efficient interleaving and forward error-correcting coding. However, estimation errors in the communication channel conditions lead to a performance loss when compared to ideal coherent demodulation of the information signal [20], [21]. Furthermore, an additional performance reduction results from the need to allocate a part of the total signal power to the pilot channel. This reduction in the voice performance is described by an overhead factor of $(1 + p_v)$, where $p_v = \kappa_{pv}/\kappa_v$ is the ratio of the pilot power to the voice power. Theoretical studies [21] show that $p_v \simeq 1/4$ is an optimal power ratio, for $R_v = 9.6$ kb/s. In this case, the pilot overhead is approximately 1 dB. A similar overhead factor is associated with the data traffic channel. The pilot overhead decreases as the data rate increases. If $p_d = \kappa_{pd}/\kappa_d$ is kept constant, more power is allocated to the pilot channel at higher data rates improving the communication channel estimate. On the other hand, if κ_{pd} is kept constant, the power ratio p_d decreases reducing the pilot overhead factor. Below, we choose to keep p_d constant and equal to p_v even though the optimal value of p_d decreases reducing the overhead factor as the data rate R_d increases.

1) Existing IS-2000 1xRTT Network: We begin by considering the performance benefit that is brought by reducing the effective noise factor of the base-station receiver in an already existing IS-2000 network with a given loading threshold X_o. The coverage considerations limit the generalized cell loading to values such that $X \leq X_o$.

(i) *Constant Data Rate* R_d. First, for a fixed data rate R_d, the capacity increase is identical to the form obtained for the IS-95 network: only the generalized loading factor, Eq. (46), is used in the capacity-increase formula, Eq. (10). Thus, the realationship between the capacity utilization, the loading threshold, and the noise factor is just that shown in Fig. 1. However, in this case, the capacity increase is allocated to voice and data users in a manner such that $\Delta X_o = \Delta n/n_\infty + \Delta m/m_\infty$ remains constant.

(ii) *Unconstrained Voice Coverage Area.* Second, we examine the peak data throughput mR_d per base station without constraining the breathing of the voice coverage area. However, the number of voice users is held at a certain limiting value, which may be zero. This type of scenario would arise naturally where the cells are serving voice users that are concentrated close to the base stations. For simplicity, we assume here either that the data rates are high enough so that $p_d \ll 1$ or that the pilot overhead is independent of the data rate. A natural measure of the data throughput is given by the ratio of the data throughput mR_d to the limiting pole data throughput $m_\infty R_d$, giving the throughput factor $\mathcal{D} = m/m_\infty$. For a fixed data coverage area, we obtain

$$\frac{\Delta\mathcal{D}}{\mathcal{D}} = \left(1 - \frac{F' R_d'}{F R_d}\right) \frac{1 - X_o}{\mathcal{D}}, \tag{49}$$

where $\Delta\mathcal{D} \equiv \mathcal{D}' - \mathcal{D}$ is the change in the data throughput when the noise factor and the data rate are changed from F and R_d to F' and R_d'. For $R_d' = R_d$, it reduces to Eq. (10). If the new, higher data rate is allocated according to the relation, $R_d' = R_d(F/F')$, the data throughput will remain the same even though the data rate is increased by F/F'. For example, reducing the noise factor by a factor of 2 will double the available data rate while keeping the throughput factor $\mathcal{D}$ constant. Alternatively, a part of the benefit originating from the lower noise factor could be allocated to the data throughput by choosing to increase the data rate by a smaller amount. Note that, as the cell loading approaches unity, the increase in the data throughput becomes negligible.

An important special case is the need to increase the data rate while maintaining the same number of data users. If the noise factor F is reduced to F', the data rate is increased by

$$\frac{\Delta R_d}{R_d} = -\left(\frac{\Delta F}{F}\right) \frac{1 - X_o}{\mathcal{D} + \dfrac{F'}{F}(1 - X_o)}, \tag{50}$$

where $\Delta R_d = R_d' - R_d$ is the absolute increase in the data rate and $\Delta F = F' - F$ is the absolute reduction in the noise factor. For $\mathcal{D} \ll 1$, which describes packet-switched data or low traffic conditions, the data-rate increase becomes

$$\frac{\Delta R_d}{R_d} = -\frac{\Delta F}{F'}. \tag{51}$$

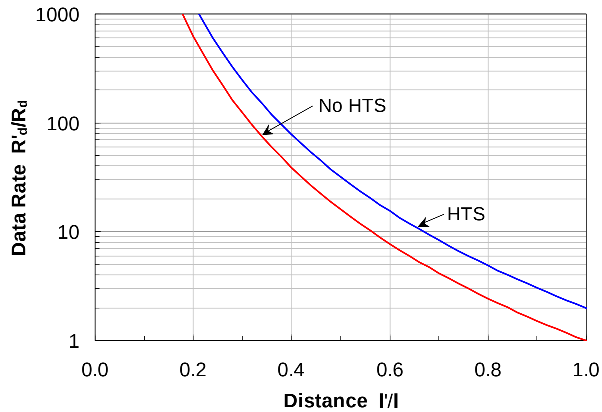

Fig. 14. The data rates with (blue line) and without (red line) an HTS front end as a function of distance for the noise factor improvement of $F/F' = 2$ and $\gamma = 4$. The data throughput per base station is constant.

A factor of two reduction in the noise factor will double the data rate under these conditions. For $\mathcal{D} \lesssim 1$, which may occur for circuit-switched data or when data traffic is high, the data-rate increase is

$$\frac{\Delta R_d}{R_d} = -\frac{\Delta F}{F}\left(\frac{1 - X_o}{\mathcal{D}}\right). \tag{52}$$

Thus, the increase in the data rate is small regardless of the noise-factor improvement, because the cell loading must necessarily be high, $X_o \sim 1$.

Typically, high data rates and throughputs are limited to users who are in close proximity to the base station. For instance, if ℓ is the radius of the base station and R_d the data rate transmitted from a user at this radius, the change in the data throughput for a user at radius ℓ' sending at a data rate R_d' is

$$\frac{\Delta\mathcal{D}}{\mathcal{D}} = \left[1 - \frac{R_d'}{R_d}\left(\frac{\ell'}{\ell}\right)^\gamma\right] \frac{1 - X_o}{\mathcal{D}}. \tag{53}$$

Here γ is the propagation exponent. Thus as the data rate increases, if one wants to keep $\mathcal{D}$ constant, the data-rate radius shrinks as

$$\frac{\ell'}{\ell} = \left(\frac{R_d}{R_d'}\right)^{1/\gamma}. \tag{54}$$

For example, if the propagation exponent $\gamma = 4$ and the data rate R_d' is increased over R_d by a factor of 10, then ℓ' would be reduced from ℓ by of order 44 %. However, if the noise factor F is reduced by the insertion of an HTS filter giving a noise factor F', then

$$\frac{\ell'}{\ell} = \left(\frac{F R_d}{F' R_d'}\right)^{1/\gamma}. \tag{55}$$

If $F/F' = 4$ (6 dB), the radius ℓ' for a 10 fold increase in the data rate will shrink by only 20 %. The data-rate dependence on the distance is illustrated for $F/F' = 2$ in Fig. 14.

(iii) *Constrained Voice Coverage Area.* Third, consider the benefit of HTS filtering on the data throughput while maintaining the voice coverage constant. In the previous section (ii) there were no limitations to the cell breathing set for voice.

Here we assume that there is a fixed number of voice and data users on the network such that $X_v \equiv \alpha_v(1+\xi)K_v n < X_o$, where X_v accounts for the interference contribution from voice channels. The network is designed so that the minimum cell radius ℓ_o is obtained for the loading factor of X_o when all users transmit voice. The maximum available data rate, which is assumed to be the same for all users transmitting data, is determined by the constraint $X_o = X_v + \mathcal{D}$, where the throughput factor $\mathcal{D} = \alpha_d(1+\xi)K_{\max} m$ coincides with our earlier definition. Therefore, the normalized maximum data rate $K_{\max} = (1+p_d)\zeta_d R_d^{\max}/W$ is

$$K_{\max} = K_v \frac{X_o - X_v}{\mathcal{D}_v}, \tag{56}$$

where $\mathcal{D}_v = \alpha_d(1+\xi)K_v m$ is the throughput factor when data users transmit at a rate of R_v. This data rate may not be accessible everywhere in the cell because of the limited handset transmit power. Indeed, users beyond the radius

$$\ell_d = \ell_o \left(\frac{K_v}{K_{\max}}\right)^{1/\gamma} \tag{57}$$

must transmit at a lower rate. For $\ell > \ell_d$, this rate is

$$K_d = K_v \frac{1 - X_v}{\mathcal{D}_v + (1 - X_o)\left(\dfrac{\ell}{\ell_o}\right)^{\gamma}}. \tag{58}$$

The maximum data rate $K_{\max}$ is only available for users at a radius $\ell \le \ell_d$ from the base station.

If the noise factor F is reduced to F' by introducing an HTS front end, the maximum available data rate is increased by

$$\frac{\Delta K_{\max}}{K_{\max}} = -\frac{\Delta F}{F}\left(\frac{1 - X_o}{\mathcal{D}}\right), \tag{59}$$

where $\Delta K_{\max} = K'_{\max} - K_{\max}$. Similarly, there is a finite radius within which this rate is supported:

$$\ell'_d = \ell_o \left(\frac{K_v}{K'_{\max}}\right)^{1/\gamma}. \tag{60}$$

Note that $\ell'_d < \ell_d$, for $F' < F$. Because of the limited available handset transmit power, for $\ell > \ell'_d$, the accessible data rate for the user is reduced from $K'_{\max}$ to

$$K'_d = K_v \frac{1 - X_v}{\mathcal{D}_v + \dfrac{F'}{F}(1 - X_o)\left(\dfrac{\ell}{\ell_o}\right)^{\gamma}}. \tag{61}$$

The data throughput increase is linearly proportional to the data rate increase: $\mathcal{D}'/\mathcal{D} = K'_d/K_d = R'_d/R_d$.

The requirement of a fixed number of data users m can be relaxed when all data users are within the radius ℓ'_d. In this case, the transmit power available for the voice channel is the limiting factor rather than that of the data users. Under these conditions, Eq. (59) can be generalized to a form where both the number of data users and rate are variable:

$$\Delta\mathcal{D} = -\frac{\Delta F}{F}(1 - X_o). \tag{62}$$

Note that here a data throughput increase is obtained for a fixed voice coverage area.

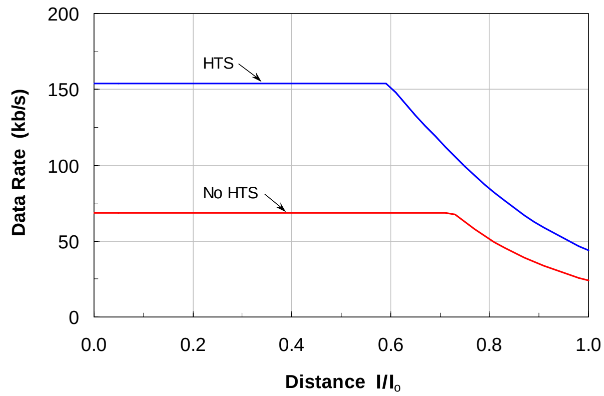

Fig. 15. The data rate R_d with (blue line) and without (red line) an HTS front end as a function of distance for 16 voice and 12 data users. The noise factor improvement due to the HTS front end is assumed to be $F/F' = 2$ and $\gamma = 4$. The other parameters are $X_o = 0.5$, $\alpha_v = 0.5$, $\alpha_d = 0.25$, $\xi = 0.55$, $p_v = p_d = 1/4$, $\zeta_v = 4$ dB, and $\zeta_d = 1$ dB, yielding $X_v = 0.3$, and $\mathcal{D}_v = 0.056$.

As an example, consider a network designed for $X_o = 0.5$, and assume that there are 12 voice and 2 data users. Then, $\mathcal{D}_v = 0.06$ and $X_v = 0.25$, and the difference $X_o - X_v$ is available for data. Here, $\xi = 0.55$, $\zeta_v = 4$ dB, $\zeta_d = 1$ dB, and $p_v = 1/4$. In this case, if $F/F' = 2$, the data rate is more than doubled close to the base station ($\ell \le \ell'_d$) and increased by approximately 81 % at the cell edge; see Fig. 15.

2) IS-2000 1xRTT Overlay on an IS-95 Network: The migration from IS-95 to IS-2000 using existing base stations is affected by new target E_b/N_o values. Currently, in IS-95, $\zeta_v \simeq 7$ dB is a typical value, yielding $K \simeq -14$ dB, for $R_v = 9.6$ kb/s. While it remains to be seen what the actual operating systems can achieve, present estimates suggest that new coding and use of the pilot channel for coherent demodulation will reduce the required value of ζ_v by of order 3 to 4 dB. For $\zeta_v = 4$ dB, κ_v is decreased to -17 dB. For $p_v = 1/4$, the reverse pilot-channel overhead is 1 dB. Thus, in IS-2000, $K_v \simeq -16$ dB. This estimate implies that the loading factor would increase for voice traffic by migrating from IS-95 to IS-2000 alone. Note that the enhanced reverse link will increase the pole capacity and the voice capacity utilization. However, the forward-link pole capacity is expected to increase even more because of such improvements as fast power control, dynamic soft handoff, and transmit diversity [16].

B. 1xEV-DO

1xEV-DO is a high rate packet data system which is a part of the CDMA2000 family of air interface specifications [22]. It has a coherent reverse link whose physical channels are orthogonalized by Walsh functions. The reverse channel structure consists of the access channel and the reverse traffic channel. They both have a pilot channel. In addition to the pilot channel, the reverse traffic channel has a reverse rate indicator (RRI) channel, a data rate control (DRC) channel, an acknowledgement (ACK) channel, and a data channel. The RRI information is time-division multiplexed with the pilot channel on the same Walsh function and transmitted at the

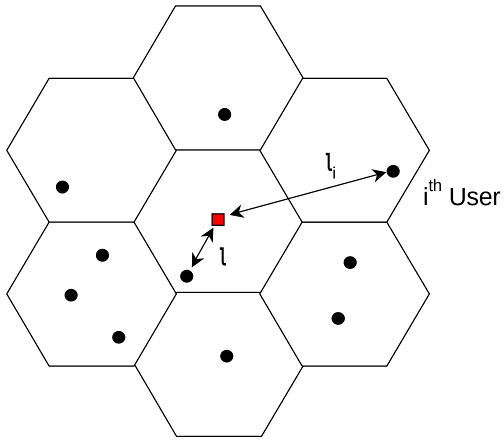

Fig. 16. Part of a 1xEV-DO network where the reverse-link communication is scheduled so that only one user per cell transmits data at any given time. The user of interest is located at a distance ℓ from its intended base station, shown by a square; the distance between that base station and the ith user in a surrounding cell is denoted by ℓ_i ($i = 1, 2, \ldots$). The number of users in each surrounding cell is Poisson distributed.

same power. Because the processing gains of the RRI, DRC, and ACK channels are large relative to the data channel, the gain of the data channel relative to the other channels must also be large for high data rates.

Because the forward link is designed to maximize the data throughput, the base station transmits data at full power to a single mobile user at any given time. While, in principle, the reverse link could also follow time-division scheduling, in the following, we assume that code-division scheduling is adopted for the reverse link. Specifically, we consider the peak data rate that is available to a single user located at a distance ℓ from the base station in its cell. The cell is in the middle of a large network, as shown in Fig. 16. The number of users in each of the surrounding cells is assumed to be Poisson distributed and these users are assumed to transmit at full power in an opportunistic scheduling fashion. User sessions generate bursty traffic characterized by packet calls that consist of several data packets [19], [23]. Intermittent packet transmissions are modeled as a dichotomic Markov process α_i where the data activity factor α_d is the probability that a packet is being transmitted by the ith user. Possible data services are Web browsing, messaging, file transfer, multimedia services, and electronic mail with multimedia attachments (image, sound, video). Each service class has its own characteristic reverse-link data activity factor.

The reverse peak data rate available for the user of interest is given by

$$\kappa_d = \frac{C(\ell)}{C(\ell) + \sum_i \alpha_i C(\ell_i) + F N_{\text{in}}} - \kappa_o, \tag{63}$$

where $\kappa_o = \sum_k \kappa_k$ takes into account the RRI, DRC, ACK, and pilot channels. Here we assume that either the data rates are large enough so that $\kappa_d \gg \kappa_o$ or κ_o is included in κ_d as a constant overhead factor. $C(\ell)$ is the received power at the base station from the user of interest transmitting data with the rate R_d such that $\kappa_d = \zeta_d R_d / W$. $C(\ell_i)$ is the received power at the same base station from the ith user in a surrounding cell and the number of users m per cell sending data packets is Poisson distributed with the average value of A_d. In order to maximize their data throughput, all users are transmitting at full power. If the 1xEV-DO network is overlayed on an existing IS-95 network with a cell radius of ℓ_o and loading factor X_o, the received power $C(\ell)$ is

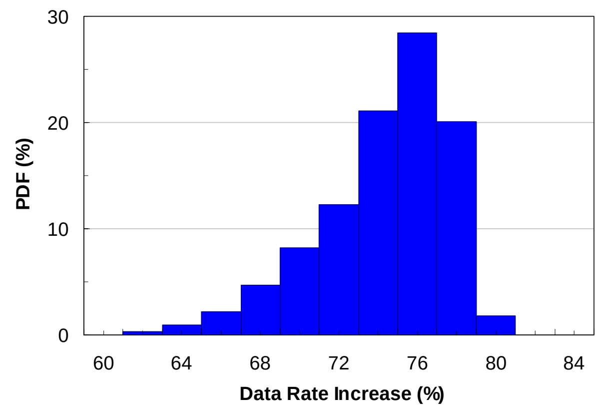

Fig. 17. The probability distribution function of the data rate increase caused by a noise-factor improvement of $F/F' = 2$ (3 dB) due to the HTS front. Here, $X_o = 0.5$, $\ell/\ell_o = 0.9$, $A_d = 10$, $\alpha_d = 0.1$, and $\gamma = 4$.

$$C(\ell) = C_o \left(\frac{\ell_o}{\ell}\right)^\gamma, \tag{64}$$

with

$$C_o = F N_{\text{in}} \frac{K}{1 - X_o}. \tag{65}$$

Assuming a uniform distribution of users in the surrounding cells,

$$\sum_i \langle \alpha_i C(\ell_i) \rangle = C_o \frac{2\alpha_d A_d}{\gamma - 2}, \tag{66}$$

it follows from Eq. (63) that the average data rate can be approximated as

$$\kappa_d = \left(\frac{\ell_o}{\ell}\right)^\gamma \frac{1}{\left(\frac{\ell_o}{\ell}\right)^\gamma + \frac{2\alpha_d A_d}{\gamma - 2} + \frac{1 - X_o}{K}}. \tag{67}$$

By lowering the noise figure of the base-station receiver from F to F', the data rate increases to

$$\kappa_d' = \left(\frac{\ell_o}{\ell}\right)^\gamma \frac{1}{\left(\frac{\ell_o}{\ell}\right)^\gamma + \frac{2\alpha_d A_d}{\gamma - 2} + \frac{1 - X_o}{K}\frac{F'}{F}}. \tag{68}$$

Thus, the HTS front end delivers a performance benefit

$$\frac{\kappa_d'}{\kappa_d} = \left(\frac{F}{F'}\right) \frac{1 + \Lambda}{1 + \Lambda \frac{F}{F'}}, \tag{69}$$

where

$$\Lambda = \left[\left(\frac{\ell_o}{\ell}\right)^\gamma + \frac{2\alpha_d A_d}{\gamma - 2}\right] \frac{K}{1 - X_o}. \tag{70}$$

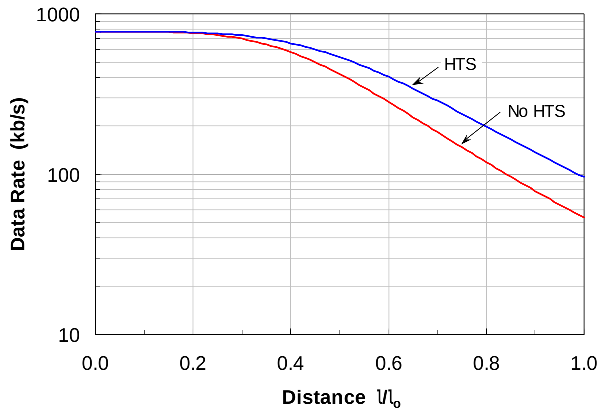

Fig. 18. The average data rates with (blue line) and without (red line) HTS front end as a function of distance relative to the cell radius ℓ_o for $X_o = 0.5$. The noise factor improvement due to the HTS front end is assumed to be $F/F' = 2$, $A_d = 10$, $\alpha_d = 0.1$, and $\gamma = 4$.

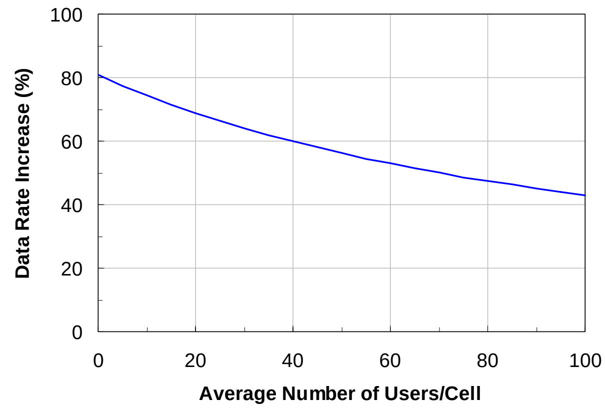

Fig. 19. The data-rate increase for a single user as a function of average number of users per cell A_d in the surrounding cells for a noise-factor improvement of $F/F' = 2$ (3 dB) due to the HTS front. Here, $X_o = 0.5$, $\ell/\ell_o = 0.9$, $\alpha_d = 0.1$, and $\gamma = 4$. The number of users is Poisson distributed.

For a user close to the cell boundary, $\ell \simeq \ell_o$, and $\alpha_d \langle m \rangle \leq 1$, the parameter $\Lambda \ll 1$ and $\kappa'_d/\kappa_d \simeq F/F'$.

As an example, let $X_o = 0.5$, $\gamma = 4$, and $\ell = 0.9\ell_o$. The analytical result, Eq. (69), predicts that the peak data rate is increased by a factor of 1.72 for a noise-factor improvement of $F/F' = 2$. By a numerical simulation, with the same parameters and using 2000 random samples for the surrounding user locations, the average data-rate increase factor $\langle \kappa'_d/\kappa_d \rangle$ is found to be 1.74. The histogram of the data-rate increases is shown in Fig. 17. The probability of increasing the data rate more than 80 % is 85 % in this case. The average data rates as a function of the radius from the base station based on the same simulation are shown in Fig. 18. As the distance from the base station decreases, the non-orthogonality factor is likely to decrease. Our simulation result would therefore underestimate the benefit of HTS front ends close to the base station. Finally, the data-rate increase is shown in Fig. 19 as a function of the average number of users per cell in the surrounding cells. Even for $A_d = 40$, the peak data rate increases by 60 % when the noise factor is halved.

VII. Final Remarks

Superconducting (HTS) filters and cryocooled low-noise amplifiers (LNA) provide new base-station receiver hardware with enhanced out-of-band interference protection and in-band amplification with exceptionally low degradation of the in-band signal-to-noise ratio. Here we have investigated the benefits that this technology brings to the reverse link in wireless CDMA networks. The key parameter characterizing this benefit is the reduction in the effective noise factor ΔF of the base-station receiver when the HTS-LNA front end replaces the conventional front end. A direct measure of ΔF is the dB reduction in handset transmit power when the HTS-LNA front end is inserted. With other network factors remaining constant, this change in the transmit power provides a simple and robust measure of this important parameter.

The mean-field analysis discussed in Section III assumes a deterministic traffic load and perfect power control so that the reverse link signals transmitted from each mobile user in a cell arrive at the base station receiver at the same power level. The carrier signals from mobiles in other cells are treated by multiplying this same power level by a reuse factor. In addition, the propagation characteristic of a cell are modeled by a propagation exponent γ. Within this model, we examined the relationship between the cell size ℓ and the loading factor X_0 as well as data rate and loading, focusing on how the receiver noise factor F entered these relations. In general, such relationships are model-dependent, however there are several results which have a more universal form and like the measurement of ΔF should be robust. In particular, the relative increase in loading threshold $\Delta X_o/X_o$ given by Eq. (10) is such a relation. If the noise factor F of the existing base-station receiver is known, a measurement of the change in handset power of a mobile when the HTS-LNA front end is inserted along with X_o should provide a direct measure of the relative increase in cell loading $\Delta X_o/X_o$ that can be achieved. This, of course, assumes that the factor limiting network performance is associated with the reverse link.

We have also extended the mean-field analysis to discuss CDMA2000 modes 1xRTT and 1xEV-DO and found similar improvements. In particular, the ratio of the change in the data throughput $\Delta\mathcal{D}$ to the existing through-put $\mathcal{D}$ given by Eq. (49) is a robust prediction and depends only upon ΔF, the data rates R_d and R'_d, and the cell loading X_o. Likewise, the maximum available data rate increase given by Eq. (59) depends directly on ΔF and the voice and total loadings X_v and X_o.

In typical reverse-link limited situations ($X_o \sim 0.5$), a 3-dB decrease in the base-station receiver noise figure will approximately increase voice capacity utilization by 50 % and packet data rates by 100 %. Additional benefits are increased coverage efficiency or a reduction in the number of required base stations. In out-of-band interference-limited situations, the reduction in the effective noise factor can be larger than 3 dB leading to enhanced benefits from HTS filtering.

While many of the other mean-field predictions depend on details of the model such as the way in which the propagation and fading is modeled, the trends with changes in ΔF should provide insight into the effectiveness of an HTS-LNA subsystem on a CDMA network. In practice, stochastic traffic associated with the varying number and spatial distribution of mobile users, the random nature of their usage and the propagation characteristics of the region makes it desirable to go beyond a mean-field analysis. Here we have discussed a numerical simulation approach which allows us to address some of these concerns and to study the dynamic interplay of the reverse link and the forward link. In particular, it allows us to make a contact with and go beyond the analytical predictions concerning the effect of IMD noise on CDMA networks. This is an important feature of numerical simulations, because IMD noise is frequently intermittent with arbitrary time scale and spatially inhomogeneous making it difficult to obtain accurate results in a general case.

The numerical simulations of the voice capacity increase associated with a reduction in the effective base-station receiver noise factor verified the mean-field results for the relative increase in capacity utilization. The simulations also provided detailed information on how the instantaneous coverage areas and the soft handoff regions changed when the normal front end of the base-station receiver was replaced by an HTS front end. A key finding from the simulations was the importance of properly optimizing the network in order to take advantage of the lower effective noise factor associated with the HTS front end. In particular, there is a need to increase the pilot and the forward-link transmission power to fully realize the HTS benefits.

ACKNOWLEDGEMENTS

We are grateful to R. Hammond, D. Chase, M. Eddy, N. Fenzi, J. Hamilton, and M. Williams for stimulating discussions.

REFERENCES

[1] M.I.Salkola, "CDMA capacity – can you supersize that?," IEEE WCNC 2002, Orlando, FL, March 2002.
[2] The noise figure in decibels (dB) is defined as $NF = 10 \lg F$, where F is the noise factor. Note that dBm is a unit of power in dB with respect to 1 mW.
[3] The reverse link refers to the mobile to base-station link and the forward link to the base-station to mobile link.
[4] K.S.Gilhousen, I.M Jacobs, R. Padovani, A.J. Viterbi, L.A. Weaver, Jr., and C.E. Wheatley III, *IEEE Trans. Veh. Technol.* **40**, 303 (1991).
[5] R.Pettai, *Noise in Receiving Systems* (Wiley, New York, 1984).
[6] A.J.Viterbi, *CDMA: Principles of Spread Spectrum Communication* (Addison Wesley, Reading, 1995).
[7] J.S.Lee and L.E.Miller, *CDMA Systems Engineering Handbook* (Artech House, Boston, 1998).
[8] Thus, D is the ratio of dropped calls to normally terminated and dropped calls.
[9] S.C.Yang, *CDMA RF System Engineering* (Artech House, Boston, 1998).
[10] N.Boucher, *Cellular Radio Handbook* (Quantum Publishing, Mill Valey, 1992).
[11] For $A_o = 60$ and the average call duration of 2 min, this would correspond to 28 hours of data collection in a real-world network.
[12] The reuse fractions ξ and ξ' are estimated for two adjacent cells using results presented in Ref. [7].
[13] The results remain essentially the same, when the effective noise factor is $F = F_o e^{\sigma_F x}$, for $x > 0$, and $F = F_o$, for $x \leq 0$.
[14] N.G. van Kampen, *Stochastic Processes in Physics and Chemistry* (North-Holland, Amsterdam, 1981).
[15] International Telecommunication Union (www.itu.int/imt).
[16] S.Willenegger, *J. of Commun. and Networks* **2**, 5 (2000).
[17] IS-2000 CDMA MC Specification.
[18] A.Saifuddin and S.Sarkar, *Proceedings of 3G Mobile Communication Technologies*, March 2000.
[19] P.Tran-Gia and K.Leibnitz, IEEE WCNC 1999, New Orleans, LA, September 1999.
[20] F.Ling, Proc. *IEEE Vehicular Technology Conf.* (VTC'93), 400 (1993).
[21] F.Ling, *IEEE Trans. Commun.* **47**, 1583 (1999).
[22] IS-856 High Rate Packet Data Air Interface Specification, 3GPP2 C.S0024, October 27, 2000.
[23] E.Anderlind and J.Zander, *IEEE Commun. Lett.* **1**, 37 (1997).